Article

Cell Host & Microbe

Supplementation with a probiotic mixture accelerates gut microbiome maturation and reduces intestinal inflammation in extremely preterm infants

Graphical abstract

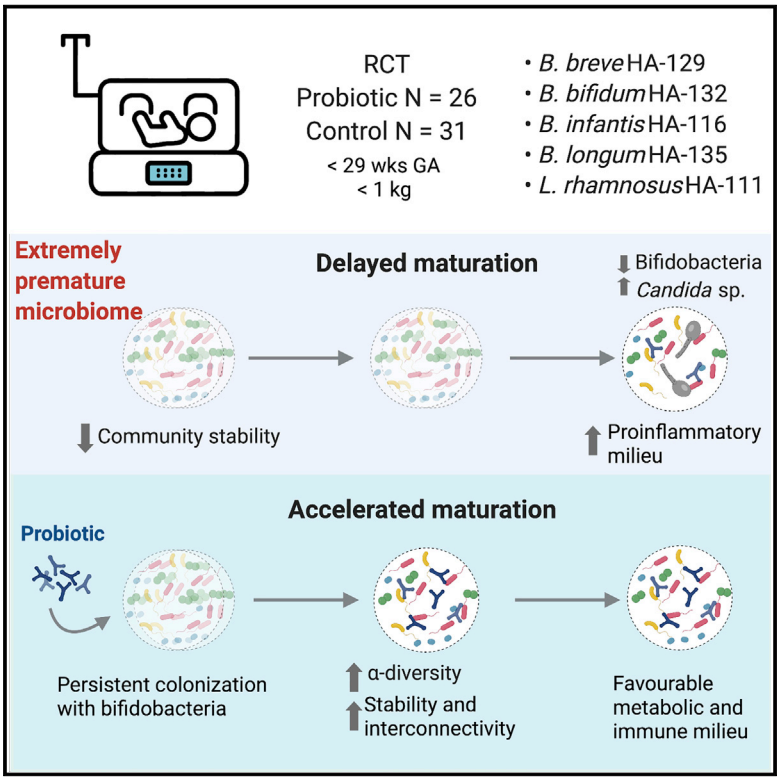

Highlights

- Multi-strain regimen accelerates microbiome maturation in extremely premature infants
- *Bifidobacterium* strains can colonize several months after administration ceases
- Bifidobacteria act as ecosystem engineers for a more mature and stable community
- Microbiome maturation is associated with a favorable metabolic and immune gut milieu

Authors

Jumana Samara, Shirin Moossavi, Belal Alshaikh, ..., Jens Walter, Harish Amin, Marie-Claire Arrieta

Correspondence

marie.arrieta@ucalgary.ca

In brief

The effects of probiotics on premature infants are not well understood. In a randomized intervention trial, Samara et al. show that a multi-strain mix accelerated microbiome maturation to resemble that of full-term infants and improved the metabolic and immune parameters, highlighting the critical ecological role of these species in early-life microbiome.

Samara et al., 2022, Cell Host & Microbe *30*, 696–711
May 11, 2022
https://doi.org/10.1016/j.chom.2022.04.005

CellPress

CellPress

Cell Host & Microbe

Article

Supplementation with a probiotic mixture accelerates gut microbiome maturation and reduces intestinal inflammation in extremely preterm infants

Jumana Samara,[1,2,3,4] Shirin Moossavi,[1,2,3,5] Belal Alshaikh,[2,6] Van A. Ortega,[1,2,3] Veronika Kuchařová Pettersen,[1,2,3,7] Tahsin Ferdous,[1,2,3] Suzie L. Hoops,[8] Amuchou Soraisham,[2,6] Joseph Vayalumkal,[2] Deonne Dersch-Mills,[2,6] Jeffrey S. Gerber,[9,11] Sagori Mukhopadhyay,[10,11] Karen Puopolo,[10,11] Thomas A. Tompkins,[12] Dan Knights,[8] Jens Walter,[13] Harish Amin,[2,6,14] and Marie-Claire Arrieta[1,2,3,14,15,*]

[1]Department of Physiology and Pharmacology, Snyder Institute for Chronic Diseases, University of Calgary, Calgary, AB, Canada
[2]Department of Pediatrics, Alberta Children's Hospital Research Institute, University of Calgary, Calgary, AB, Canada
[3]International Microbiome Centre, University of Calgary, Calgary, AB, Canada
[4]Health Sciences Centre, Winnipeg, MB, Canada
[5]Microbiome and Microbial Ecology Interest Group (MMEIG), Universal Scientific Education and Research Network (USERN), Calgary, Canada
[6]Calgary Zone Section of Neonatology, Calgary, AB, Canada
[7]Department of Medical Biology, UiT The Arctic University of Norway, Tromsø, Norway
[8]Biotechnology Institute and Department of Computer Science and Engineering, University of Minnesota, Minneapolis, MN, USA
[9]Division of Infectious Diseases, Children's Hospital of Philadelphia, Philadelphia, PA, USA
[10]Newborn Care at Children's Hospital of Philadelphia, Philadelphia, PA, USA
[11]Department of Pediatrics, University of Pennsylvania Perelman School of Medicine, Philadelphia, PA, USA
[12]Lallemand Health Solutions, Montreal, QC, Canada
[13]School of Microbiology, Department of Medicine, and APC Microbiome Ireland, University College Cork, Cork, Ireland
[14]These authors contributed equally
[15]Lead contact
*Correspondence: marie.arrieta@ucalgary.ca
https://doi.org/10.1016/j.chom.2022.04.005

SUMMARY

Probiotics are increasingly administered to premature infants to prevent necrotizing enterocolitis and neonatal sepsis. However, their effects on gut microbiome assembly and immunity are poorly understood. Using a randomized intervention trial in extremely premature infants, we tested the effects of a probiotic product containing four strains of *Bifidobacterium* species autochthonous to the infant gut and one *Lacticaseibacillus* strain on the compositional and functional trajectory of microbiome. Daily administration of the mixture accelerated the transition into a mature, term-like microbiome with higher stability and species interconnectivity. Besides infant age, *Bifidobacterium* strains and stool metabolites were the best predictors of microbiome maturation, and structural equation modeling confirmed probiotics as a major determinant for the trajectory of microbiome assembly. *Bifidobacterium*-driven microbiome maturation was also linked to an anti-inflammatory intestinal immune milieu. This demonstrates that *Bifidobacterium* strains are ecosystem engineers that lead to an acceleration of microbiome maturation and immunological consequences in extremely premature infants.

INTRODUCTION

Postnatal microbial colonization in humans results in a dynamic assembly process that establishes the gut microbiota in a series of ecological succession events (Koenig et al., 2011; Yassour et al., 2016; Rao et al., 2021). In infants born by vaginal delivery at term, early predominance of facultative anaerobic bacteria (i.e., *Streptococcus* spp., Enterobacteriaceae, and *Staphylococcus* spp.) is followed by a community dominated by *Bacteroides* and *Bifidobacterium* species that further diversifies during and after weaning (Yassour et al., 2016; Mitchell et al., 2020). This process is drastically altered in infants born prematurely, with the magnitude of alterations correlating with the severity of prematurity (Stewart et al., 2016; La Rosa et al., 2014; Korpela et al., 2018; Chernikova et al., 2018; Wandro et al., 2018; Olin et al., 2018; Arboleya et al., 2012; Costello et al., 2013). Premature infants display a gut microbiome of reduced alpha-diversity, delayed colonization with obligate anaerobic bacteria, and increased abundance in potentially pathogenic bacteria (Stewart et al., 2016; La Rosa et al., 2014; Korpela et al., 2018; Chernikova et al., 2018; Wandro et al., 2018; Olin et al., 2018; Arboleya et al., 2012; Costello et al., 2013). Despite a large degree of temporal and interindividual variability, the gut microbiome of the premature newborn follows patterns of microbial colonization that are

to some degree conserved (Rao et al., 2021; La Rosa et al., 2014; Korpela et al., 2018). For example, extremely premature infants between 24 and 28 weeks gestational age (GA) are initially colonized by a community dominated by *Staphylococcus* spp., followed by *Enterococcus* spp. predominance between 28 and 32 weeks GA. Members of Enterobacteriaceae bloom later through interactions with *Staphylococcus* spp. between 32 and 35 weeks GA (Rao et al., 2021). Following this period of facultative anaerobes predominance, strict anaerobic *Bifidobacterium* species become highly abundant at the age of term, when the premature microbiome begins to resemble the term infant composition (La Rosa et al., 2014; Korpela et al., 2018).

The ecological drivers that disrupt the gut microbiota in premature infants are insufficiently understood. It has been proposed that organ-specific immaturity of preterm infants might provide selective pressure different from that of the term infant, either selecting for specific organisms and/or constitute habitat filters that prevent the colonization of the normal pioneer colonizers of the term infant gut (Henderickx et al., 2019). Additionally, preterm infants are more likely to be born by cesarean section (C-section), receive antimicrobial treatment, achieve enteral feeding more slowly, and require longer hospitalization compared with those born at term, all of which constitute potential determinants of microbiome alterations (Laforest-Lapointe and Arrieta, 2017). The consequences of the delayed microbiome maturation are also not well understood. Microbiome development in preterm babies is strongly correlated with GA, and the maturational delays may therefore reflect adaptations of the microbiota that are specific and perhaps necessary for preterm babies. However, extremely premature infants are strongly predisposed to devastating conditions like necrotizing enterocolitis (NEC) and neonatal sepsis (Pammi et al., 2017; Masi and Stewart, 2019; Vongbhavit and Underwood, 2016), which are not only linked to an altered gut microbiome (Masi and Stewart, 2019; Stewart et al., 2016) but can further be prevented through probiotics (Bertelsen et al., 2016; Aceti et al., 2017). Given that probiotics modulate the microbiome in premature infants (Alcon-Giner et al., 2020; Plummer et al., 2018), their established benefits support a causal role for microbiome alterations as a true dysbiosis (Brüssow, 2020) in the etiology of these pathologies.

Probiotics are increasingly administered in neonatal intensive care units (NICUs) given their clinical effectiveness in reducing the risk of NEC and sepsis (Bertelsen et al., 2016; Aceti et al., 2017). However, their use remains a matter of debate (Ofek Shlomai et al., 2014; Modi, 2014), and very little is known on the effect of probiotics on the assembly process of this nascent ecosystem and infant immune status. A recent study in term infants demonstrated that *B. infantis* EVC001 stably engrafts and dominates the community (Frese et al., 2017), and supplementation induced anti-inflammatory effects in term, breastfed infants (Henrick et al., 2021). However, it is unclear if probiotics exert the same effects in extremely premature infants who present with a much higher degree of dysbiosis and are at a heightened risk of infection and acute inflammatory conditions (Pammi et al., 2017; Masi and Stewart, 2019; Vongbhavit and Underwood, 2016). In addition, healthy infants are often colonized by a mix of *Bifidobacterium* species (*B. breve*, *B. bifidum*, and *B. longum*) that can establish trophic interactions between themselves (Egan et al., 2014) and other genera (Cheng et al., 2020), which might constitute the basis for robust community assemblies early in life (Tannock, 2021).

Here, we report findings from a randomized clinical trial of 57 extremely premature infants born at less than 1,000 g birth weight and less than 29 weeks GA (clinicaltrials.gov identifier: NCT03422562) in Calgary, Canada. Twenty-six infants were randomized to a probiotic treatment (FloraBABY, Renew Life, Canada) containing four *Bifidobacterium* strains from species that are common and dominant in the infant gut (*B. breve* HA-129, *B. bifidum* HA-132, *B. longum* subsp. *infantis* HA-116 [*B. infantis* HA-116] and *B. longum* subsp. *longum* HA-135 [*B. longum* HA-135]) and *Lacticaseibacillus rhamnosus* HA-111, and 31 infants were left untreated. Before, during, and 6 months after the intervention, we determined the presence and persistence of each bacterial strain using strain-specific qPCR, evaluated the bacterial and fungal microbiome using 16S and ITS rRNA sequencing and metabolomics, and measured cytokine levels in stool. We integrated these data through ecological and statistical models to determine the consequences of probiotic use on premature microbiome assembly and intestinal immunity.

RESULTS

Bifidobacterium strains, but not *L. rhamnosus*, can stably colonize the premature infant gut

Extremely premature NICU-resident infants were randomized to receive daily administration of FloraBABY or no probiotic. Probiotic administration started during the first week after birth following the collection of the first stool sample (T1), while two fecal samples were collected during treatment (T2 and T3), followed by a 2-week washout phase at term age (T4). A final sample was collected at 6 months corrected age (CA; T5) (Figure 1A). Two infants received probiotics prior to sample collection, and thus their T1 samples were removed from the analysis. Study participant clinical and nutritional characteristics did not differ between treated and control groups (Tables S1 and S2).

Strain-specific qPCR showed increased fecal cell numbers for all strains during probiotic administration at time points T2 (2–3 weeks of age) and T3 (4–5 weeks of age) when compared with the control group (Figures 1B–1F and S2). All probiotic strains remained significantly higher in the treatment group at T4 (2 weeks after administration). At T5 (6 months CA), all *Bifidobacterium* strains except *B. infantis* HA-116 remained significantly elevated in the treatment group (Figures 1B–1F; Table S3). While several infants still harbored detectable levels of *B. infantis* HA-116 at T5, cell numbers of *L. rhamnosus* HA-111 dropped below detection levels at T5 in all infants. These findings indicate stable colonization and proliferation of all *Bifidobacterium* strains in the premature infant gut for 6 months after administration was stopped, while *L. rhamnosus* HA-111 was unable to engraft (Figure 1B). Interestingly, *B. bifidum* HA-132, *B. longum* HA-135, and *B. breve* HA-129, but not *B. infantis* HA-116 or *L. rhamnosus* HA-111, increased to detectable levels in 93%, 53%, and 71% of control infants by 6 months CA, respectively (T5; Figures 1B–1F; Table S3), suggesting that transfer of these three probiotic strains to some control infants did occur during later stages of hospitalization.

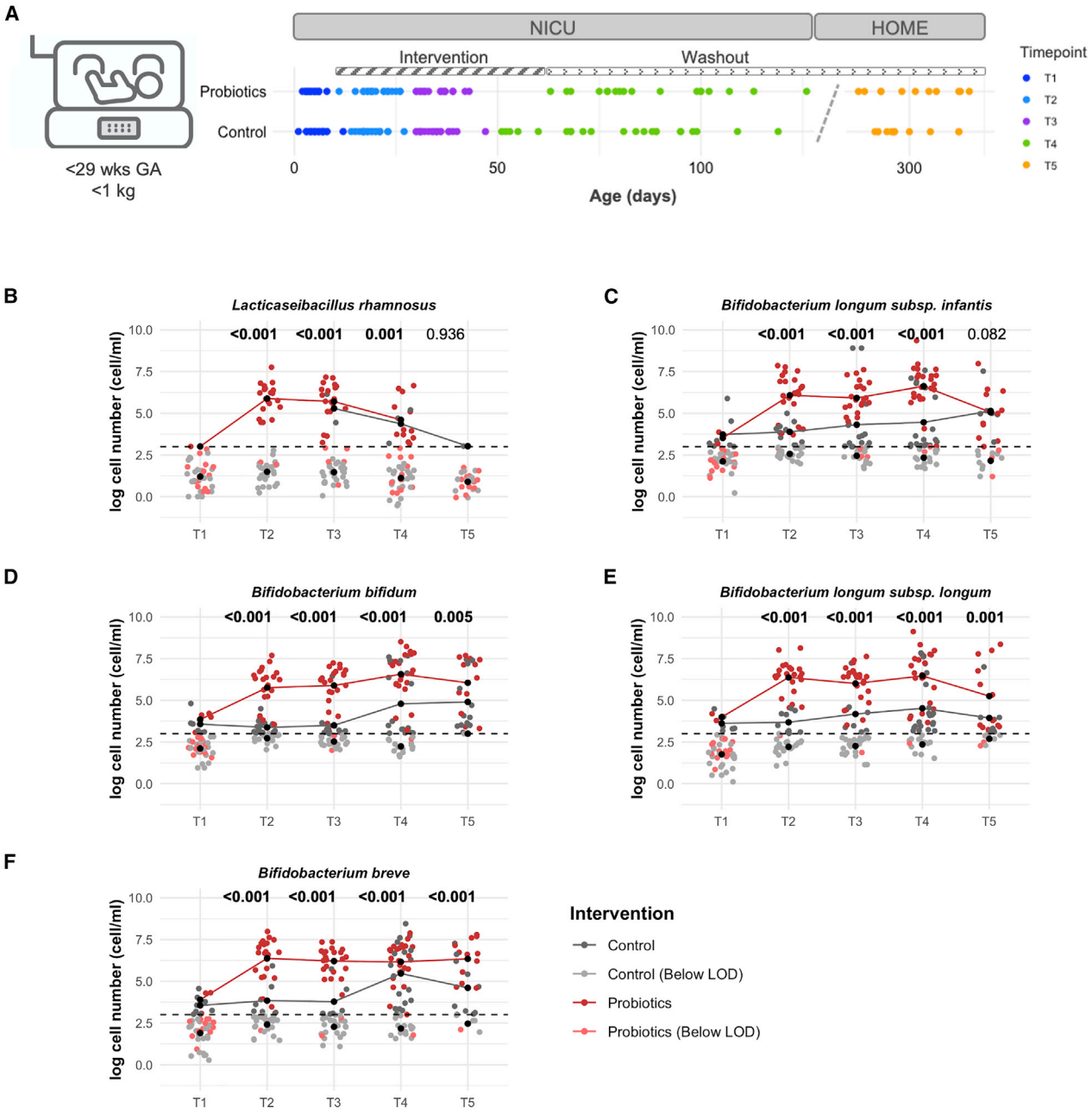

Figure 1. Probiotic *Bifidobacterium* strains can stably colonize the extremely premature infant gut

(A) Study design for the randomized controlled trial of probiotics in extremely preterm infants. In the treatment group, probiotic was started in the first week of life after a first sample collection (T1) and continued until 37–39 weeks gestational age (GA) weeks spanning T2 and T3. Additional samples were collected after cessation of probiotic at 39–40 weeks GA (T4) and 6 months corrected age (CA) (T5).

(B–F) Concentration of probiotic strains assessed by strain-specific qPCR demonstrates increased concentration of all probiotics strains immediately after starting probiotic at T2. *Lacticaseibacillus rhamnosus* decreased after cessation of probiotics (B) while the *Bifidobacterium* strains showed stable colonization until 6 months CA (C-F). The dashed line denotes the limit of detection (10^3 bacterial cells/mL). p values are obtained from linear mixed models (LMM) and post estimation for linear combination of coefficients (see also Table S2). LOD, limit of detection.

Probiotic mixture accelerates microbiome maturation in extremely premature infants to a level comparable to term infants

Previous observational studies have shown that probiotics can be used to modify the premature infant microbiome, mainly increasing alpha-diversity and the relative abundance of *Bifidobacterium* species (Alcon-Giner et al., 2020; Plummer et al., 2018). However, the ecological effects on gut microbiome assembly and successional trajectory have not been systematically determined using an intervention trial. To achieve this, we applied an unsupervised clustering approach to the microbiome data collected temporally throughout the study. This analysis

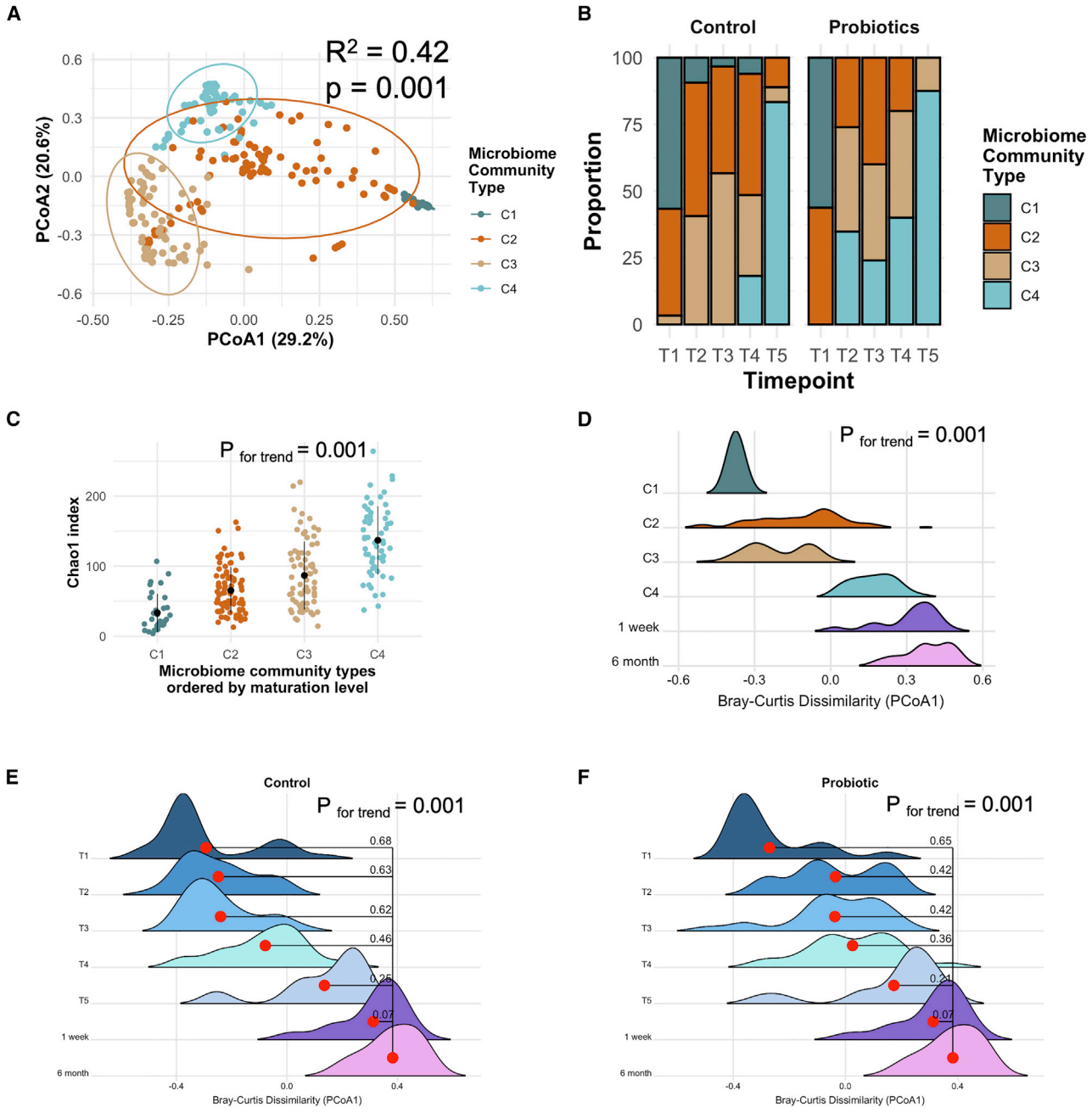

Figure 2. A probiotic mixture accelerates gut microbiome maturation in extremely preterm infants

(A) Four gut microbiome community types were identified using hierarchical clustering on Bray-Curtis dissimilarity matrix. Association of the community types with beta-diversity was tested using PERMANOVA.

(B) Microbiome community type distribution across time points and probiotic use. Community types showed temporal distribution, with C1 and C2 more frequent in earlier and C4 in later time points. As a result, C4 is considered the mature community type, which appeared earlier in infants treated with probiotics.

(C) Comparison of bacterial richness (Chao1) in community types (see Figure S2D for comparison of beta-diversity).

(D) Comparison of the maturational patterns of the microbiome community types with term infants at 1 week and 6 months of age.

(E and F) Comparison of the temporal development of preterm infant microbiome with term infants at 1 week and 6 months of age in controls (E) and probiotic-treated infants (F). Centroid of each time point is denoted as the red circle, and the distance to the centroid of each timepoint to the centroid of 6-month term infants are presented as labels. Trend analysis in (C)–(F) were conducted using trendyspliner in SplinectomeR package.

revealed four microbiome community types (C1–C4) (Figures 2A and S3A). Community type C1 and C2 dominated at T1, while C4 is completely absent at T1 but dominated at T5 (Figure 2B). There was a gradual increase in alpha diversity (Chao1) and community homogeneity as the microbiota matured from C1 to C4 (Figures 2C and S3D). Furthermore, C4 community type is

characterized by high levels of *Bifidobacterium* while the less mature community types are dominated by *Staphylococcus* and *Enterobacteriaceae* (Figure S4C), reflecting preceding succession stages in microbiome development (Koenig et al., 2011; Yassour et al., 2016; Rao et al., 2021).

To determine to what degree the community types detected in preterm infants differ to the microbiome of term infants, we compared them to microbiomes from 1 week (N = 44) and 6 months (N = 24), breastfed infants born at term. Ordination analysis based on Bray-Curtis dissimilarity showed that while the overall composition of the premature microbiome differed from term infants (Figure S4A), microbiomes from community type C4 showed substantial overlap (on PCoA1) with the microbiome of term born infants (Figures 2D and S4B). These findings establish that the community types detected in premature infants represent gradual stages of maturation of the gut microbiota that range from an immature microbiome to one that more closely resembles that of term infants, which we define as a mature microbiome in extremely premature infants.

An analysis of the impact of probiotics on community maturation revealed that there was no difference in community type distribution between the probiotics and control groups before treatment started during the first week of life (T1), with both groups consisting of C1 and C2 in equal proportions (Figure 2B). During the treatment period, which spanned from 2 to 6 weeks of age (T2–T3), community type C1 transitioned to C2 or C3 in both groups, but there was a proportion of infants that transitioned to C4 exclusively in the probiotics group (Figure 2B). Infants in both control and probiotic groups predominantly consisted of C4 community type at 6 months CA (T5; Figure 2B). While the control group exhibited a delayed maturational pattern of gut microbiome similar to what has been previously described in premature infants (Korpela et al., 2018; La Rosa et al., 2014; Rao et al., 2021), 36% of the infants who received probiotics arrived at the mature C4 community as early as T2 compared with none of the controls (Figures S3B and S3C). This acceleration in microbiome maturation through the probiotic treatment was also seen in the Bray-Curtis analysis, where the average dissimilarity to full-term microbiomes was lower at time points T2 ($p < 0.001$), T3 ($p < 0.001$), and T4 ($p = 0.014$) when compared with term breastfed infants, demonstrating restoration of the community (Figures 2E and 2F).

Probiotics promote a community with higher species interconnectivity and stability

Primary succession patterns in macro- and microbial ecology often follow an increase in community diversity and interaction network complexity (Young et al., 2005). In accordance, we observed increased species richness as clusters transitioned (Figure 2C). To further assess community ecological parameters, we determined interconnectedness, complexity, stability, and probabilities of transition between community types.

Network analysis revealed that interconnectivity increased from C1 to C4 (Figures 3A and 3C). This ecological shift is strongly influenced by the probiotic intervention with a higher community interconnectivity in the treatment group as compared with the untreated controls (Figure 3B). Markov chain analysis to determine the probability of transitions between community types revealed that both the probability of the community to mature to C4, as well as to remain as C4, was higher in the probiotic group, indicative of higher community stability (Figure 3D). A time-to-event analysis confirmed that infants who were supplemented with probiotics showed a higher probability to mature to C4 earlier than controls and that these effects persist beyond cessation of the probiotic (Figure 3E). Finally, a multivariate logistic regression analysis showed that the impact of probiotics on the acceleration of microbiome maturation was more prominent than that of infant age, and other factors identified as microbiome-modulating factors in early life, including birth mode, feeding, and antibiotics (Laforest-Lapointe and Arrieta, 2017) (Figure 3F). Together, this analysis indicates that probiotic supplementation to premature infants accelerates microbiota assembly toward a more mature and stable microbiome.

Probiotics accelerates gut metabolome maturation in extremely premature infants

We carried out untargeted metabolomics on a subset of fecal samples (N = 82) to compare the intestinal metabolic milieu between infants who received probiotics and controls. Using permutational multivariate analysis of variance (PERMANOVA) on Bray-Curtis dissimilarities among samples, we identified that infant age and probiotics had strong effects on the premature infant metabolome composition, with sampling time point and probiotic intervention explaining 26.3% and 6.7% of the metabolome variance, respectively ($p < 0.001$; Figures 4A and 4B). We also identified differences in temporal metabolic transition influenced by probiotic intervention and confirmed an interaction effect between time point and probiotic use on the metabolome (PERMANOVA, $R^2 = 8.4\%$, $p = 0.03$; Figure 4A). We observed a transition in the metabolome as time points increased, which was accelerated in infants who received probiotics (Figure 4B). All but T1 samples clustered together in the probiotic group, in contrast to control samples, in which the transitions were more temporally distinct. This suggests that this probiotic intervention not only accelerated the transition to a more mature microbiome composition but also resulted in a more mature metabolic state.

To determine the metabolic characteristics of a mature microbiome in preterm infants, we compared the fecal metabolome of C4 (N = 25) infants with that of the immature states (C1–C3, N = 27). Microbiome maturation (C4) made a significant contribution to variation in metabolome composition ($R^2 = 7.3\%$, $p < 0.001$; Figure 4C). Out of the 82 metabolites measured, we identified 14 differential metabolites as significantly different (fold change > 2, false discovery rate [FDR] $p < 0.05$) (Figure 4D; Table S4). These included elevated levels of the essential amino acids leucine, valine, and phenylalanine, and the fatty acids oleic acid, palmitoleic acid, and arachidic acid in samples categorized as immature, suggesting the presence of nutritional substrates that remain unutilized by the immature microbiome and/or the premature gut.

We also compared the metabolic profiles of the immature and mature microbiome in preterm infants with those of infants born at term (N = 30). Among the 14 metabolic features that differentiated mature and immature community states in preterm infants, 8 metabolites in the mature microbiome preterm group reached similar levels to term infants (Figure 4E). These included an increase in cholate and taurine in the mature microbiome composition. Cholate is a primary bile acid produced in high concentrations in the liver, and when conjugated with taurine forms

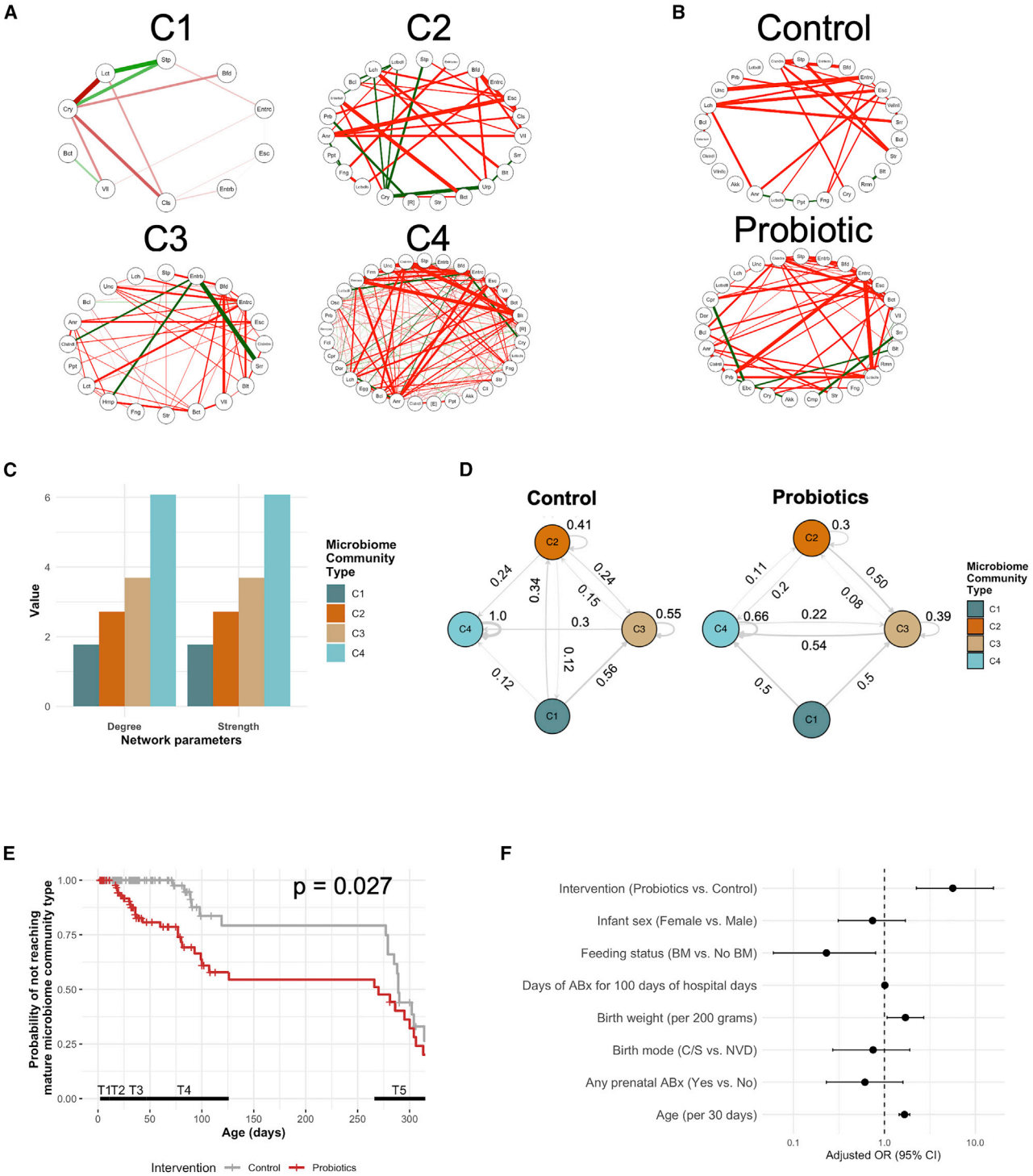

Figure 3. A probiotic mixture promotes a microbial community with higher interconnectivity and stability

(A and B) Network analysis of the preterm infant microbiome along the microbiome maturation trajectory (A) and by intervention (B).

(C) Comparison of network degree and strength across community types.

(D) Probability of transition between community types assessed by Markov chain modeling compared in controls and probiotic group.

(E) Time-to-event analysis demonstrates that probiotics accelerates transition into the C4 mature community type. Kaplan-Meier curve for the probability of not reaching the mature community type is shown.

(F) Multivariable logistic regression demonstrating the association of probiotic treatment with microbiome maturation independently of early-life events. Adjusted odds ratio (OR) and 95% confidence interval (CI) are presented for all variables in the model.

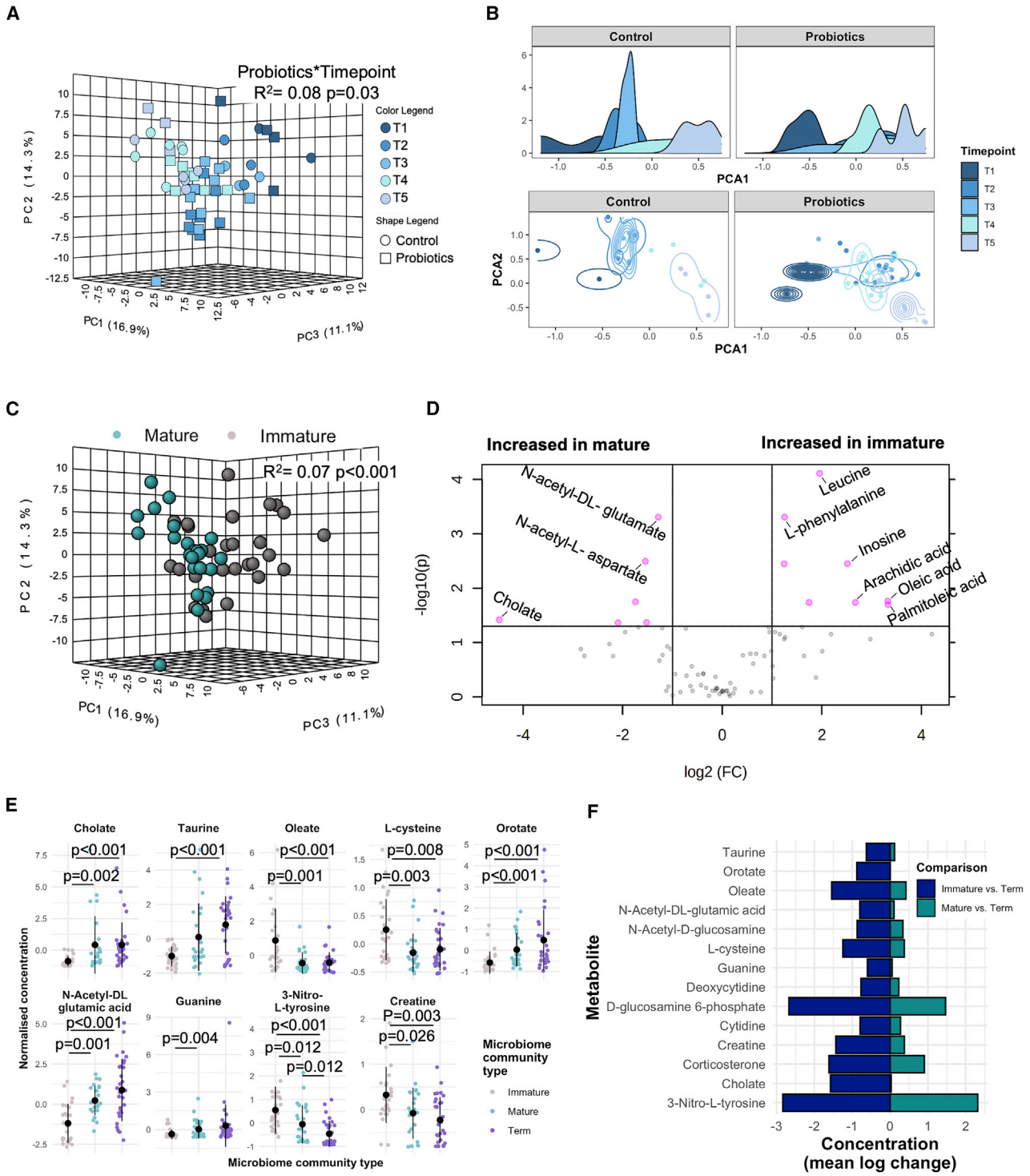

Figure 4. *Bifidobacterium*-induced microbiome maturation is reflected in the stool metabolome

(A and B) Principal component analysis of gut metabolome in premature infants at different time points and by intervention. Interaction between the effects of timepoint and probiotics was tested using PERMANOVA.

(C) Principal component analysis of gut metabolome in premature infants with mature (C4) versus immature (C1–C3) community types. Effect of maturational status on the variance of the metabolome was tested using PERMANOVA.

(D) Differentially enriched metabolites in mature (C4) versus immature (C1–C3) community types as assessed by volcano plot with fold-change threshold of 2 and adjusted t test threshold of 0.05. Pink circles represent features above this threshold.

(legend continued on next page)

taurocholic acid, the highest concentrated bile acid in bile (Ridlon et al., 2016). Critical for fat digestion and absorption, bile acids are typically reduced in serum and duodenal aspirates in premature infants, and they increase with post-natal age (Boehm et al., 1997). A mature microbiome composition also resulted in reduced levels of oleic acid (Figure 4E), the fatty acid found in highest concentration in breast milk (Ramiro-Cortijo et al., 2020), suggesting improved fat absorption, potentially from increased bile acid production in premature infants with a mature microbiome composition. We also detected a decrease in 3-nitrotyrosine linked to the mature microbiome composition, which approximated levels detected in term infants (Figure 4E). This metabolite is an established marker of cell damage, inflammation, and nitric oxide production, and it is elevated in a large number of pathological inflammatory diseases (Murata and Kawanishi, 2004), including prematurity-related pathologies such as pulmonary dysplasia (Banks et al., 1998; Sheffield et al., 2006) and NEC (Egan et al., 2016), further supporting the benefits of microbiome maturation in the intervention group.

L-cysteine, an important substrate for bifidobacteria (which are auxotroph for it; Ferrario et al., 2015), was reduced in the mature microbiomes (Figure 4E), which may reflect L-cysteine consumption by microbial communities with a greater *Bifidobacterium* abundance. We also detected elevated levels of guanine, *n*-acetyl-DL-glutamic acid, and reduced creatine linked to microbiome maturity and reaching comparable levels to those in term infants (Figure 4E), which may also be the result of bifidobacteria. An increase in guanine and *n*-acetyl-DL-glutamic acid and a decrease in creatine were found in the stool of breastfed term infants compared with those fed formula (Chow et al., 2014; Li et al., 2020), which correlated with the abundance of bifidobacteria (Li et al., 2020). These findings provide evidence for increased functional similarity between the mature preterm microbiome to that of the term breastfed babies, which are not explained by differences in breastmilk intake, as they were similar in the probiotic and control groups (Tables S3 and S4). Finally, when comparing metabolite levels using features with the largest differences according to maturation state (highest fold-change values), the mature preterm samples more closely approximated the term metabolome than the immature preterm samples (Figure 5F). Altogether, these findings indicate that microbiome maturation in preterm infants results in potentially beneficial metabolic changes with important similarities to the intestinal metabolic milieu of healthy, breastfed infants born at term.

Bifidobacterial probiotic strains and metabolites drive microbiome maturation

To determine the drivers of microbiome maturation, we applied a random-forest classifier to identify variables that can predict maturation to community type C4 (versus C1–C3), and their relative importance. We included variables known to be major drivers in microbiome assembly (Laforest-Lapointe and Arrieta, 2017), such as host (age, GA, and sex), clinical (peri- and post-natal antibiotics and birth mode), dietary (breast[milk] feeding, hydrolyzed protein formula, and fortification), as well as microbiome variables (probiotic strains cell numbers and probiotic duration) and differential fecal metabolites as variables for predictions. Apart from the infants chronological age, which was the best predictor, levels of creatine, taurine, guanine, *n*-acetyl-DL-glutamic acid, and cell numbers of the probiotic *Bifidobacterium* strains constituted the most important factors predicting gut microbiome maturation status (Figure 5A), showing higher Gini indices than factors often considered important, such as antibiotic treatment, birth mode, breastfeeding, and GA. The *L. rhamnosus* HA-111 strain grouped lower than these factors, further suggesting a lower effect of this strain in microbiome maturation in this clinical trial.

We also used structural equation modeling (SEM) to incorporate a theoretical framework of causal pathways underlying the associations between study variables and the premature gut microbiome (Figure 5B). Only time points T1–T4 were included in the model due to the reduced number of samples collected at T5 and the necessity to include complete sample numbers at each time point for SEM. We selected variables with a reported effect on the infant microbiome (Laforest-Lapointe and Arrieta, 2017), including birth mode, GA at birth, antibiotic use, breast milk intake, and probiotic use. Given the widespread use of breast milk instead of formula at the NICU where the study took place, breast milk intake could only be evaluated at T2, at a time when some of the infants received formula.

SEM analysis revealed that C-section and GA at birth were directly associated with bacterial richness at T1 ($\beta = -0.48$; $p < 0.001$ and $\beta = -0.28$; $p = 0.04$, respectively). Breast milk intake was directly associated with T2 richness ($\beta = 0.17$; $p = 0.006$), yet a more prominent effect was observed for probiotics at T2 ($\beta = 0.595$, $p < 0.001$). Although probiotics were being administered at both T2 and T3, the effect on microbiome richness (Chao1) was not significant at the T3, yet microbiome composition at T2 strongly impacted subsequent communities' richness at T3 and T4 ($\beta = 0.74$; $p < 0.001$ and $\beta = 0.62$; $p < 0.001$, respectively; Figure 5B). This intriguing observation suggests that by impacting microbiome composition at an early time point (T2), probiotics may contribute to the trajectory of microbiome assembly, possibly through priority effects (Martínez et al., 2018). Similar significant effects were also made for alpha-diversity (Shannon index; not shown). Overall, these findings, together with the facts that probiotics persisted long after consumption ceased (Figure 1B) and that duration was not a strong predictor of microbiome maturation in the random-forest model (Figure 5A), challenging the requirement of long-term probiotic administration to achieve compositional changes in the microbiome of extreme premature infants.

Probiotic use depletes *Candida* spp., but probiotic-*Candida* interactions do not modulate microbiome maturation

Given that multi-kingdom microbe-to-microbe interactions have been identified as drivers of the assembly process (Rao et al.,

(E) The most discriminatory metabolic features from immature (gray) or mature (turquoise) microbiome maturation status in premature infants compared with term, breastfed infants (purple). Comparisons were made by pairwise Wilcoxon test.
(F) Metabolite levels by microbiome maturity in relation to term breastfed infants. Mean fold difference in the mature-term versus immature-term comparisons are shown.

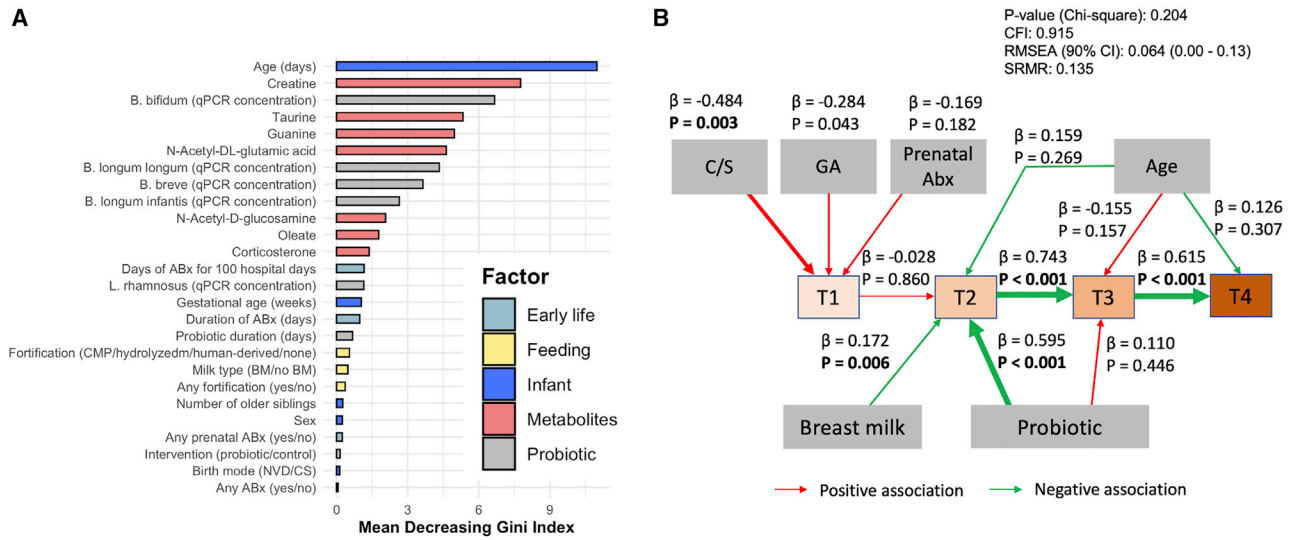

Figure 5. Probiotic strains and stool metabolites are predictive and drivers of microbiome maturation

(A) Predictors of mature microbiome community type (C4 versus C1, C2, and C3 combined) ordered by their importance identified through random-forest modeling using 10-fold cross-validation, 500 trees, and 1,000 permutations.

(B) Structural equation modeling was used to differentiate the influence of probiotics on bacterial richness (Chao1) at each time point while taking into account the structure of association of other early-life factors. Probiotic was administered during T2 and T3 time points. Model fit was assessed using p value, CFI, RMSEA, and SRMRs. Abx, antibiotics; CFI, comparative fit index; C/S, cesarean section; RMSEA, root mean square error of approximation; SRMRs, standardized root mean residuals.

2021), we studied the temporal changes of the premature mycobiome and its association with probiotic use. Compared with what has been established for the bacterial microbiome (La Rosa et al., 2014; Korpela et al., 2018), temporal analysis of the premature gut mycobiome did not reveal major shifts in the relative abundance of the most abundant fungal genera between T1–T4 (Figure 6A). Community typing also identified four fungal clusters, yet these did follow distinct patterns of community transition (Figures S5A and S5B), suggesting that the gut mycobiome may not display community maturation patterns in the same manner as bacterial communities. Probiotic administration resulted in a significant decrease in the relative abundance of *Candida* spp. (Figures 6A and 6B), in agreement with previous studies (Hu et al., 2017; Manzoni et al., 2006). While many samples had low relative abundance of *Candida* spp. in our study, more samples were dominated by very high levels of *Candida* spp. in the infants who did not receive probiotics (Figure 6C). When categorizing at a 50% relative abundance threshold, the proportion of samples from infants with >50% *Candida* spp. abundance was significantly lower in the intervention group (Figure 6D), indicating that probiotic use induces a strong anti-*Candida* effect.

We assessed the specific role of *Candida* spp. as a modulator of the effect of probiotic use on gut microbiome maturation. We used SEM to evaluate the direct influence of *Candida* spp. abundance on bacterial richness (Figure 6E), as well as its indirect role on microbiome maturation via interactions with probiotic strains (Figure 6F). While probiotics and milk type were significantly associated with the gut microbiome richness, we did not observe a direct association of *Candida* spp. with bacterial richness in this model (Figure 6E). Similarly, the association of probiotic strains with bacterial community types was not influenced by the relative abundance of *Candida* spp. (Figure 6F), denoting the stronger ecological influence of the probiotic strains compared with endogenous *Candida* spp. The strong anti-*Candida* effect of the probiotics may explain why this fungal species is not associated with the successional patterns observed in our study, as it was in a recent thorough ecological analysis of the premature microbiome assembly without a probiotic intervention (Rao et al., 2021). Although the effect of the probiotic on *Candida* spp. does not seem to constitute a mechanism by which microbiota maturation is enhanced, the effect is nevertheless important given the clinical relevance of *Candida* spp. in nosocomial infections among premature infants (Hu et al., 2017; Manzoni et al., 2006).

Probiotic-induced microbiome maturation reduced proinflammatory cytokines in the stool of extremely premature infants

Extremely premature infants are at an increased risk of NEC, a devastating inflammatory condition (Pammi et al., 2017; Masi and Stewart, 2019; Vongbhavit and Underwood, 2016). To investigate the effect of probiotics on intestinal inflammation, we determined the concentration of 17 cytokines and calprotectin in stool in a subset of samples (N = 170). Cytokines play a central role in immune and inflammatory functions in the gut and are known to accumulate in stool and reflect intestinal inflammatory processes (Saiki et al., 1998). We applied generalized estimation equation models on longitudinal data to determine differences in stool cytokines during the time of hospitalization and after the probiotic intervention started (T2–T4). Probiotics led to an overall reduction in several important proinflammatory cytokines, including calprotectin, IFN-γ, IL-12p70, IL-4, as well as an increase in IL-22 (Figure 7A). In the gut, IL-22 exerts generally

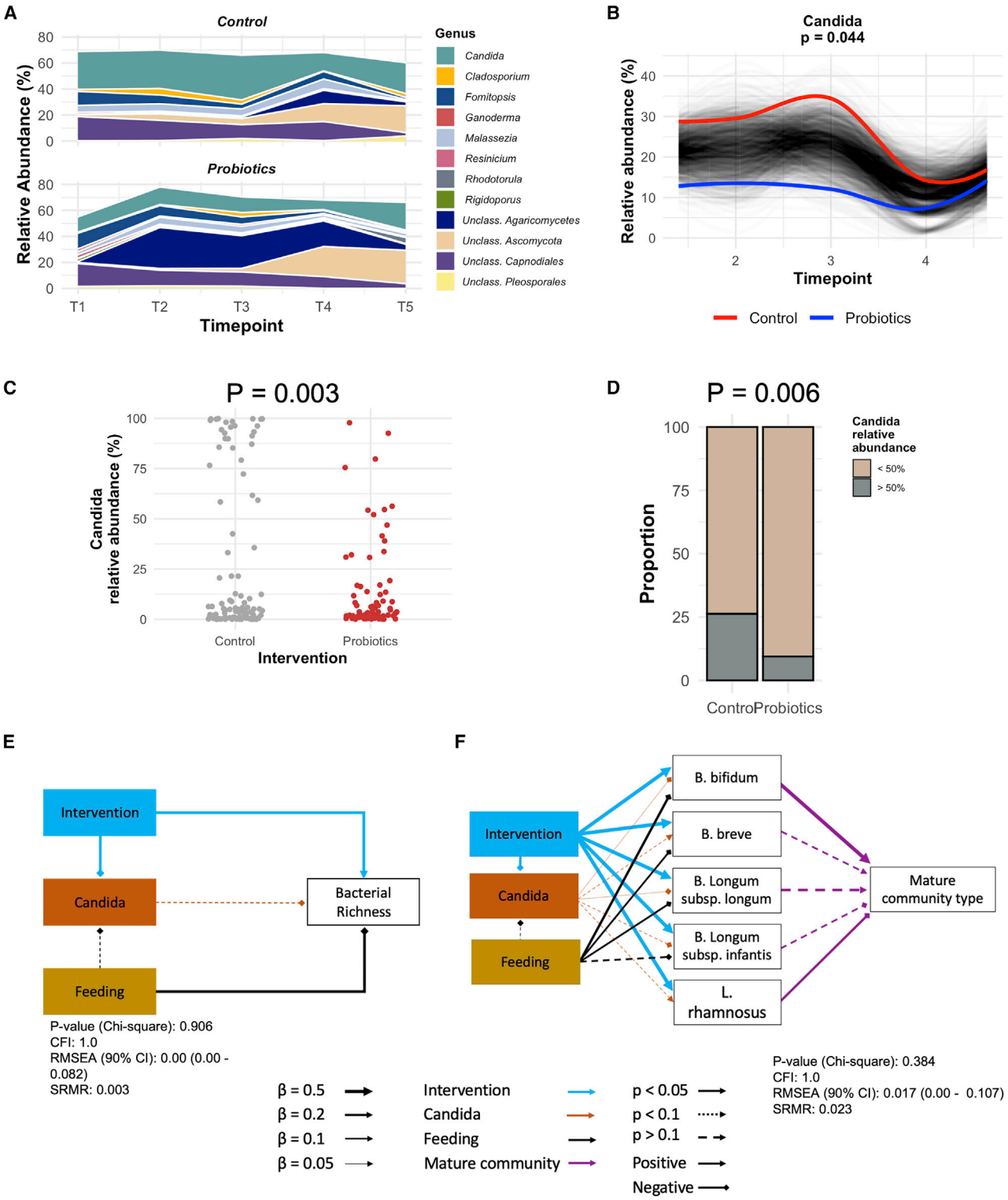

Figure 6. A probiotic mixture depletes *Candida* spp., but its interactions with *Candida* do not modulate microbiome maturation

(A) Mycobiome community structure at genus level compared in controls and infants who received probiotics.

(B) Longitudinal analysis of *Candida* spp. according to the intervention using splinectomeR reveals significantly lower abundance in the probiotic group.

(C) Distribution of *Candida* spp. by intervention confirms lower average relative abundance in the probiotic group.

(D) Categorizing *Candida* spp. relative abundance into <50% or >50% revealed the infants who received probiotic are less frequently dominated by high levels of *Candida* spp.

(legend continued on next page)

protective functions, such as maintaining barrier function and tissue injury regeneration (Dudakov et al., 2015), with recently reported critical role in the prevention and treatment of NEC in mice (Mihi et al., 2021). This demonstrates a strong and consistent intestinal anti-inflammatory effect of probiotics in extremely premature infants (Figure 7A; Table S5).

We also compared cytokine levels in relation to microbiome maturation (C4 versus C1–C3 versus term). There was a significant decrease in IFNγ, IL-1β, and IL-8 and calprotectin in stool samples from preterm infants with a mature microbiome composition compared with those with an immature microbiome composition, and the levels of IFNγ and IL-1βa in the mature microbiome were similar to those detected in term infant stool samples (Figure S6). Overall, the differences between the immune status of preterm and term infants were significantly smaller for infants harboring the mature microbiome type (C4) than those with more immature microbiomes (C1–3) (Figure 7C). Finally, correlation analysis between cytokine concentrations and microbial abundances revealed numerous significant correlations. Pathobionts, specifically the genera *Staphylococcus* and *Streptococcus*, showed positive correlations, while cell numbers of the probiotic strains showed negative correlations with the majority of the immune factors measured (Figure 7B). These findings suggest a predominant role of the probiotic strains on the immune milieu detected in stool samples from extremely premature infants.

DISCUSSION

Microbiome maturation is disrupted and delayed in preterm infants predisposing the infant to life-threatening pathologies (Pammi et al., 2017; Masi and Stewart, 2019; Vongbhavit and Underwood, 2016). Our work demonstrated that a probiotic formulation leads to the stable colonization of *Bifidobacterium* strains weeks before bifidobacteria become dominant members of the fecal microbiome in untreated preterm infants (Korpela et al., 2018; La Rosa et al., 2014). This is in line with what was recently reported by Alcon-Gener et al. (Alcon-Giner et al., 2020) in an observational study, showing strong and persistent colonization by *B. bifidum* after supplementation to preterm infants born at <32 weeks GA (Alcon-Giner et al., 2020). Our study further revealed that probiotics expedited transition to a more mature and stable community state, two key features of later stages of primary succession (Connell and Slatyer, 1977). We define this as a bifidobacteria-high community with enhanced stability and species interconnectivity that more closely resembles that of healthy, breastfed, and vaginally born term infants. Cell numbers of the *Bifidobacterium* strains administered with the probiotic and stool metabolites were among the strongest predictors of maturation, providing a mechanistic link between probiotic administration and an acceleration of microbiome maturation to a state more closely resembling the vaginally born, breastfed infant microbiome, the current benchmark for a desired term infant microbiome (Laforest-Lapointe and Arrieta, 2017).

Probiotic-induced microbiome maturation was also accompanied by metabolic and immune features that may be beneficial to this infant population. This includes changes to features previously associated with NEC in premature infants, including oleate (Lee et al., 2001), proinflammatory cytokines (Cho et al., 2016; Maheshwari et al., 2014), and 3-nitrotyrosine (Egan et al., 2016). Overall, the mature microbiome composition resulted in marked metabolic and immune differences that approximated the term stool metabolome (Figures 4D and 7B) and is indicative of improved fatty acid absorption, breastmilk metabolism, and reduced inflammation. Our findings complement the recently reported immune silencing effect of the probiotic *B. infants* EVC001 on term infants (Henrick et al., 2021), extending the evidence for *Bifidobacterium* strains as drivers of beneficial immune imprinting during early life. These findings, as well as the ecological attributes of the more mature and stable microbiome, suggest a beneficial effect to extremely premature infants, especially considering the well-established role of bifidobacteria excluding pathogenic organisms or providing cues for the developing immune system (O'Callaghan and van Sinderen, 2016).

The pronounced effects of probiotic administration on microbiome maturation can be explained using an ecological framework. To establish in the gut, organisms must first overcome the habitat filters present and then possess traits to acquire the available resources to become competitive (Walter et al., 2018). In contrast to many other probiotic products, the probiotic used in this study is composed of *Bifidobacterium* strains from autochthonous species that naturally dominate the early-life microbiota of infants (O'Callaghan and van Sinderen, 2016; Tannock, 2021). Such strains, in contrast to *L. rhamnosus* HA-111, are highly adapted to the infant gut. These adaptation include the ability to utilize human milk oligosaccharides and sugar hexoses (O'Callaghan and van Sinderen, 2016), to competitively exclude other microbes, including pathogens through short-chain fatty acid production (Fukuda et al., 2011), to decrease the intestinal luminal pH (O'Callaghan and van Sinderen, 2016), and to sustain metabolic cross-feeding of other gut microbiome species (Falony et al., 2006; Belenguer et al., 2006). Our random-forest analysis revealed that all *Bifidobacterium* strains (but not *L. rhamnosus* HA-111) contributed to microbiome maturation, suggesting a contribution of the wider *Bifidobacterium* community to microbiome assembly. The strongest predictor among the bifidobacteria, *B. bifidum*, provides substrates (fucose and sialic acid) from the hydrolysis of mucus and HMOs to other microbiome members (Centanni et al., 2019; Egan et al., 2014; Gotoh et al., 2018), while the weakest predictor, *B. infantis*, internalizes substrates without sharing (Tannock, 2021), supporting a contribution of cross-feeding in microbiome maturation. Our findings further point to the importance of priority effects in that an earlier arrival of the probiotic strains enhances both their own persistence and modifies the trajectory of the assembly process (Sprockett et al., 2018; Martínez et al., 2018). Given the rapid and sustained ecosystem transformation linked to the probiotic *Bifidobacterium* strains, we propose that bifidobacteria act as ecosystem engineers (Laforest-Lapointe and Arrieta, 2017) in

(E and F) Structural equation modeling to examine the direct effect of *Candida* spp. on bacterial richness (E) and indirect effect on microbiome maturation via interaction with probiotic strains (F). Model fit was assessed using p value, CFI, RMSEA, and SRMR. CFI, comparative fit index; C/S, cesarean section; RMSEA, root mean square error of approximation; SRMRs, standardized root mean residuals.

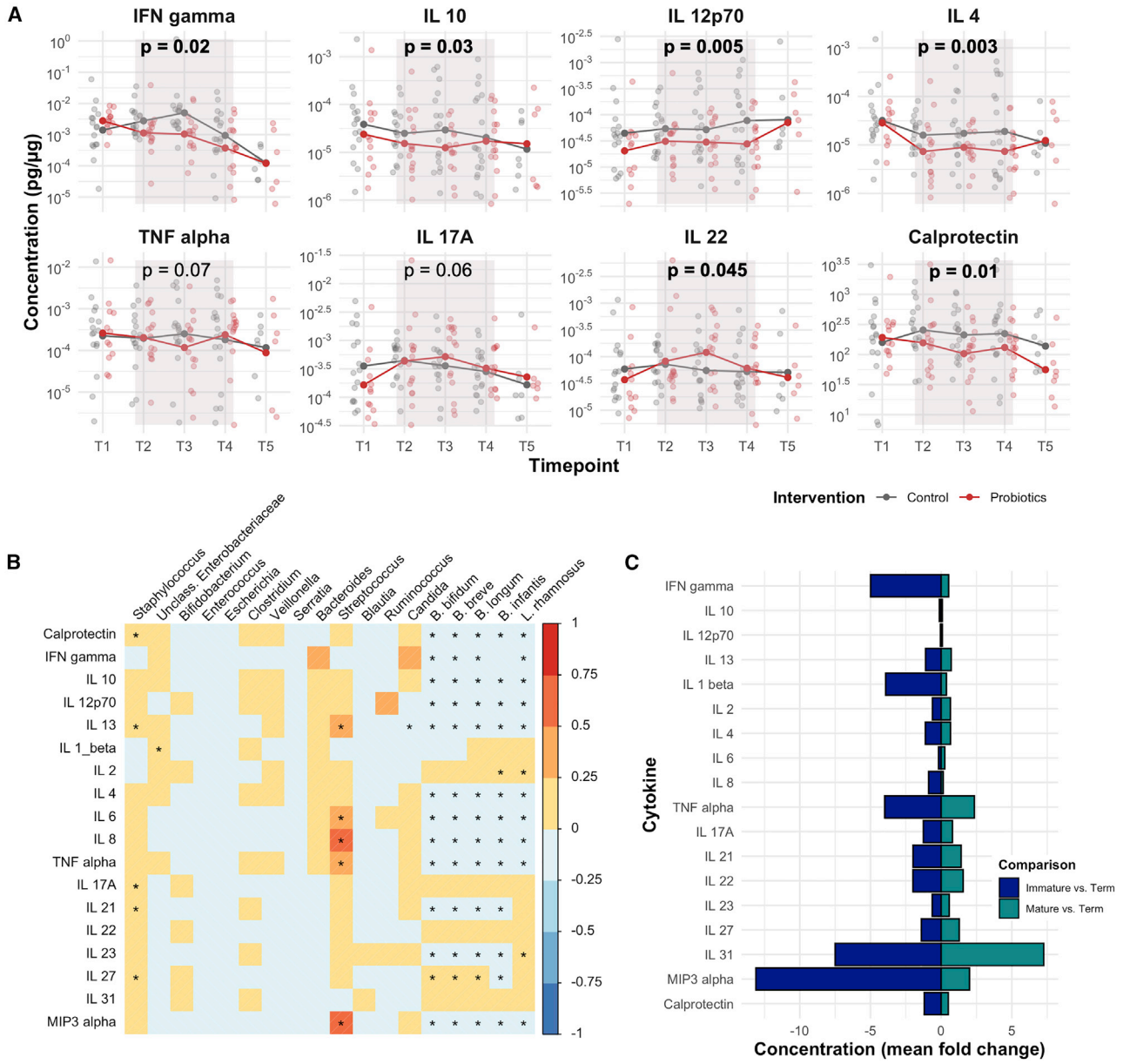

Figure 7. A probiotic mixture-induced microbiome maturation reduced proinflammatory cytokines in stool of extremely premature infants

(A) Cytokine concentrations in premature infants according to the intervention. Comparisons were made by generalized estimating equation (Table S5).

(B) Correlation of fecal cytokine levels with the 12 most abundant bacterial genera (mean relative abundance > 1%), *Candida*, and probiotic strains log 10 transformed cell numbers. Statistical significance was assessed by adjusting for multiple comparison using Benjamini and Hochberg method.

(C) Cytokine levels by microbiome maturity in relation to term breastfed infants. Mean fold difference in the mature-term versus immature-term comparisons are shown.

the premature microbiome, capable of building, transforming, and preserving the microbial habitat in the infant gut.

Apart from providing strong evidence for the ability to use probiotics to restore the microbiome in preterm infants, our findings provide important clues on the ecological factors that lead to the pronounced disruptions observed in preterm microbiomes (Stewart et al., 2016; La Rosa et al., 2014; Korpela et al., 2018; Chernikova et al., 2018; Wandro et al., 2018; Olin et al., 2018; Arboleya et al., 2012; Costello et al., 2013). Our findings show that autochthonous *Bifidobacterium* strains can effectively and stably colonize the preterm gut. In addition, our random-forest analysis and SEM showed that such strains and metabolites associated with their predominance in the community are more important determinants of microbiome maturation than the host, clinical, and dietary factors often considered to play important roles. This suggests that the premature microbiome is not primarily disrupted through treatments and feeding practices of a modern NICU, or the premature physiological or immunological state of the host, and that microbiome maturational delays are unlikely to reflect necessary adaptations of the microbiota

to the premature conditions. Instead, our findings point to the inability of the premature infant to acquire the necessary strains to initiate the assembly process. Additional research is warranted to unravel the ecological mechanisms by which bifidobacteria, whether one or multiple strains, drive a richer a more stable microbial community early in life.

Ecologically, the human gut microbiota can be viewed as a meta-community in which individuals are linked through dispersal, which constitutes a key ecological process that shapes microbiome assembly at local scales (Walter and Ley, 2011). Our strain-specific quantification showed that some infants in the control group did acquire the probiotic strains (Figure 1), likely because they were housed in the same NICU, demonstrating the ability to acquire early colonizers through horizontal transmission. However, this only occurred in a smaller subset of infants, and most infants acquired strains them later in microbiome development. These findings demonstrate that dispersal occurs infrequently in an NICU, possibly due to hygienic barriers to prevent infections, as well as the clinical practices linked to preterm births that disrupt vertical transmission from the mother to the infant (c-sections, antibiotics, maternal separation, etc.), all of which can reduce exposure to pioneer organisms that colonize term infants. This dispersal barrier may also contribute to immune dysregulation resulting in increased intestinal inflammation, which is central to the pathogenesis of inflammatory and infectious pathologies in extremely premature infants. If probiotics contain the right microbes that have evolved as early colonizers in humans, they can essentially function as a mechanism to restore the dispersal process. In this context, probiotics fall within the framework of ecological restoration as an attempt to reach a desired community, or to avoid an undesirable one. The findings of this study show that such an approach has great potential for clinical applications with potential health benefits to very vulnerable infant population.

Limitations of the study

Our study is limited by its size, as it was not powered to capture health outcomes in this population, such as NEC or sepsis. Larger and prospective studies in premature infants are needed to confirm if the metabolic and immune benefits resulting from an accelerated microbiome maturation result in improved health outcomes in extremely premature infants during infancy and later in life. Given that conditions such as NEC are driven by inflammation, such knowledge has substantial clinical implications. While we accounted and controlled for most of the variables known to influence the infant microbiome, other factors, such as breastmilk composition and maternal diet, were not included. In addition, blood collection was not possible in this critical clinical setting, which better reflects host immune status. Finally, while bifidobacterial are a feature predominant strain in most infant populations worldwide (Arrieta et al., 2018; Partida-Rodriguez et al., 2021; de Goffau et al., 2022; Ayeni et al., 2018; De Filippo et al., 2010), there may be exceptions to this. For example, a report from South Korea showed that bifidobacteria are less abundant members of the initial infant microbiome (Lee et al., 2015). Another report found that although *bifidobacteria* was the dominant group in a cohort of Gambian and Malawian infants, they did not observe any correlation between bifidobacterial and health outcomes (Davis et al., 2017). Thus, our concept of microbiome maturation for extremely preterm should be contextualized to the socio geographical factors known to influence the composition of the infant microbiome.

STAR★METHODS

Detailed methods are provided in the online version of this paper and include the following:

- KEY RESOURCES TABLE
- RESOURCE AVAILABILITY
  - Lead contact
  - Materials availability
  - Data and code availability
- EXPERIMENTAL MODEL AND SUBJECT DETAILS
  - Inclusion and exclusion of study participants
  - Maternal, infant and early-life factors
- METHOD DETAILS
  - Sample collection and processing
  - DNA extraction
  - Quantitative PCR
  - 16S rRNA and ITS2 gene sequencing
  - Metabolomics
  - Immune factor determination
- QUANTIFICATION AND STATISTICAL ANALYSIS
  - Sequencing processing
  - Assessing sequencing technical accuracy
  - Exclusion of data
  - Probiotic *strain* colonization assessment
  - Identification of microbiome community types
  - Assessment of the effect of probiotics on the transition to the mature community type
  - Comparison of microbiome composition in preterm with term infants
  - Ecological investigation of microbiome community in response to probiotics
  - Metabolomics comparison by intervention and community type
  - Predictive modelling
  - Structural equation modelling
  - Longitudinal analysis
  - Univariate analysis of cytokines and metabolites
- ADDITIONAL RESOURCES

SUPPLEMENTAL INFORMATION

Supplemental information can be found online at https://doi.org/10.1016/j.chom.2022.04.005.

ACKNOWLEDGMENTS

The authors would like to acknowledge study participants and their families for their support to research, as well as NICU nurses for their effort in sample collection and communication with the study group. The following collaborators supported clinical and laboratory aspects of this research: Rachel Sheinfeld, Erik van Tilburg Bernardes, Mackenzie Gutierrez, Kristen Kalbfleisch, Julia Gorospe, Amanda Piano, Dr. Neha Bansal, Marija Drikic, and Ryan Groves. This work was supported by funds from the Cumming School of Medicine, the Alberta Children Hospital Research Institute, the Snyder Institute of Chronic Diseases, the Canadian Institutes for Health Research. The International Microbiome Center is supported by the Cumming School of Medicine,

University of Calgary, Western Economic Diversification and Alberta Economic Development, and Trade, Canada. S. Moossavi is supported by CIHR and Killam Postdoctoral Fellowship. V.A.O. is supported by a MITACS Elevate Fellowship. J.W. acknowledges support by Science Foundation Ireland (SFI) through an SFI Professorship (19/RP/6853) and a Centre award (APC/SFI/12/RC/2273_P2) to the APC Microbiome Ireland.

AUTHOR CONTRIBUTIONS

H.A., B.A., A.S., J.V., and D.D.-M. contributed to the design of the premature RCT study. J.S. and B.A. monitored the clinical trial. J.S. communicated with study participant families, conducted study interviews, and compilated all clinical data. J.S., V.K.P., and V.A.O. prepared all the samples for sequencing and metabolomics analysis. J.S. carried out qPCR analysis. S. Moossavi, J.S., and M.-C.A. analyzed the 16S and ITS2 sequences. S. Moossavi, J.S., V.A.O., and V.K.P. analyzed the metabolomics data. S. Moossavi and T.F. carried out statistical analysis. V.A.O. performed immune and protein determination assays. S. Moossavi and M.-C.A. created the paper figures. T.A.T. provided probiotic strains and with J.W., guidance on qPCR protocol. S.L.H., D.K., J.S.G., S. Mukhopadhyay, and K.P. provided the 16S sequences from the MAGIC Study. M.-C.A., S. Moossavi, J.S., and J.W. contributed to data interpretation and writing the first and subsequent drafts of the manuscript. All authors edited the manuscript and contributed extensively to the work presented here.

DECLARATION OF INTERESTS

T.A.T. was the Research Director at Lallemand Health Solutions, the manufacturers of FloraBABY. The other authors declare no competing interests.

Received: November 29, 2021
Revised: February 8, 2022
Accepted: April 11, 2022
Published: May 11, 2022

REFERENCES

Aceti, A., Maggio, L., Beghetti, I., Gori, D., Barone, G., Callegari, M.L., Fantini, M.P., Indrio, F., Meneghin, F., Morelli, L., et al. (2017). Probiotics prevent late-onset sepsis in human milk-fed, very low birth weight preterm infants: systematic review and meta-analysis. Nutrients *9*, 904.

Alcon-Giner, C., Dalby, M.J., Caim, S., Ketskemety, J., Shaw, A., Sim, K., Lawson, M.A.E., Kiu, R., Leclaire, C., Chalklen, L., et al. (2020). Microbiota supplementation with *Bifidobacterium* and *Lactobacillus* modifies the preterm infant gut microbiota and metabolome: an observational study. Cell Rep. Med. *1*, 100077.

Arboleya, S., Binetti, A., Salazar, N., Fernández, N., Solís, G., Hernández-Barranco, A., Margolles, A., de Los Reyes-Gavilán, C.G., and Gueimonde, M. (2012). Establishment and development of intestinal microbiota in preterm neonates. FEMS Microbiol. Ecol. *79*, 763–772.

Arrieta, M.C., Arévalo, A., Stiemsma, L., Dimitriu, P., Chico, M.E., Loor, S., Vaca, M., Boutin, R.C.T., Morien, E., Jin, M., et al. (2018). Associations between infant fungal and bacterial dysbiosis and childhood atopic wheeze in a nonindustrialized setting. J. Allergy Clin. Immunol. *142*, 424–434.e10.

Ayeni, F.A., Biagi, E., Rampelli, S., Fiori, J., Soverini, M., Audu, H.J., Cristino, S., Caporali, L., Schnorr, S.L., Carelli, V., et al. (2018). Infant and adult gut microbiome and metabolome in rural Bassa and urban settlers from Nigeria. Cell Rep. *23*, 3056–3067.

Banks, B.A., Ischiropoulos, H., Mcclelland, M., Ballard, P.L., and Ballard, R.A. (1998). Plasma 3-nitrotyrosine is elevated in premature infants who develop bronchopulmonary dysplasia. Pediatrics *101*, 870–874.

Bartoń, K. (2020). MuMIn: multi-model inference. R package version 1.43.17. https://CRAN.R-project.org/package=MuMIn.

Bates, D., Maechler, M., Bolker, B., and Walker, S. (2015). Fitting linear mixed-effects models using lme4. J. Stat. Softw. *67*, 1–48.

Belenguer, A., Duncan, S.H., Calder, A.G., Holtrop, G., Louis, P., Lobley, G.E., and Flint, H.J. (2006). Two routes of metabolic cross-feeding between *Bifidobacterium* adolescentis and butyrate-producing anaerobes from the human gut. Appl. Environ. Microbiol. *72*, 3593–3599.

Bertelsen, R.J., Jensen, E.T., and Ringel-Kulka, T. (2016). Use of probiotics and prebiotics in infant feeding. Best Pract. Res. Clin. Gastroenterol. *30*, 39–48.

Boehm, G., Braun, W., Moro, G., and Minoli, I. (1997). Bile acid concentrations in serum and duodenal aspirates of healthy preterm infants: effects of gestational and postnatal age. Biol. Neonate. *71*, 207–214.

Brüssow, H. (2020). Problems with the concept of gut microbiota dysbiosis. Microb. Biotechnol. *13*, 423–434.

Callahan, B.J., Mcmurdie, P.J., Rosen, M.J., Han, A.W., Johnson, A.J., and Holmes, S.P. (2016). DADA2: high-resolution sample inference from Illumina amplicon data. Nat. Methods *13*, 581–583.

Caporaso, J.G., Lauber, C.L., Walters, W.A., Berg-Lyons, D., Huntley, J., Fierer, N., Owens, S.M., Betley, J., Fraser, L., Bauer, M., et al. (2012). Ultra-high-throughput microbial community analysis on the Illumina HiSeq and MiSeq platforms. ISME J, 1621–1624.

Centanni, M., Ferguson, S.A., Sims, I.M., Biswas, A., and Tannock, G.W. (2019). *Bifidobacterium bifidum* ATCC 15696 and *Bifidobacterium breve* 24b metabolic interaction based on 2′-*O*-fucosyl-lactose studied In steady-state cultures in a Freter-style chemostat. Appl. Environ. Microbiol. *85*. e02783–18.

Cheng, C.C., Duar, R.M., Lin, X., Perez-Munoz, M.E., Tollenaar, S., Oh, J.H., Van Pijkeren, J.P., Li, F., Van Sinderen, D., Gänzle, M.G., and Walter, J. (2020). Ecological importance of cross-feeding of the intermediate metabolite 1,2-propanediol between bacterial gut symbionts. Appl. Environ. Microbiol. *86*. e00190-20.

Chernikova, D.A., Madan, J.C., Housman, M.L., Zain-ul-Abideen, M., Lundgren, S.N., Morrison, H.G., Sogin, M.L., Williams, S.M., Moore, J.H., Karagas, M.R., and Hoen, A.G. (2018). The premature infant gut microbiome during the first 6 weeks of life differs based on gestational maturity at birth. Pediatr. Res. *84*, 71–79.

Cho, S.X., Berger, P.J., Nold-Petry, C.A., and Nold, M.F. (2016). The immunological landscape in necrotising enterocolitis. Expert Rev. Mol. Med. *18*, e12.

Chow, J., Panasevich, M.R., Alexander, D., Vester Boler, B.M., Rossoni Serao, M.C., Faber, T.A., Bauer, L.L., and Fahey, G.C. (2014). Fecal metabolomics of healthy breast-fed versus formula-fed infants before and during in vitro batch culture fermentation. J. Proteome Res. *13*, 2534–2542.

Clasquin, M.F., Melamud, E., and Rabinowitz, J.D. (2012). LC-MS data processing with MAVEN: a metabolomic analysis and visualization engine. Curr. Protoc. Bioinformatics. Chapter 14, Unit14 11.

Connell, J.H., and Slatyer, R.O. (1977). Mechanisms of succession in natural communities and their role in community stability and organization. Amer. Natur. *111*, 1119–1144.

Costello, E.K., Carlisle, E.M., Bik, E.M., Morowitz, M.J., and Relman, D.A. (2013). Microbiome assembly across multiple body sites in low-birthweight infants. mBio *4*. e00782–e00713.

Daróczi, G., and Tsegelskyi, R. (2018). pander: An R 'Pandoc' Writer. R package version 0.6.3. https://CRAN.R-project.org/package=pander.

Davis, J.C., Lewis, Z.T., Krishnan, S., Bernstein, R.M., Moore, S.E., Prentice, A.M., Mills, D.A., Lebrilla, C.B., and Zivkovic, A.M. (2017). Growth and morbidity of Gambian infants are influenced by maternal milk oligosaccharides and infant gut microbiota. Sci. Rep. *7*, 40466.

De Filippo, C., Cavalieri, D., Di Paola, M., Ramazzotti, M., Poullet, J.B., Massart, S., Collini, S., Pieraccini, G., and Lionetti, P. (2010). Impact of diet in shaping gut microbiota revealed by a comparative study in children from Europe and rural Africa. Proc. Natl. Acad. Sci. USA *107*, 14691–14696.

De Goffau, M.C., Jallow, A.T., Sanyang, C., Prentice, A.M., Meagher, N., Price, D.J., Revill, P.A., Parkhill, J., Pereira, D.I.A., and Wagner, J. (2022). Gut microbiomes from Gambian infants reveal the development of a non-industrialized Prevotella-based trophic network. Nat. Microbiol. *7*, 132–144.

Dudakov, J.A., Hanash, A.M., and Van Den Brink, M.R. (2015). Interleukin-22: immunobiology and pathology. Annu. Rev. Immunol. *33*, 747–785.

Egan, C.E., Sodhi, C.P., Good, M., Lin, J., Jia, H., Yamaguchi, Y., Lu, P., Ma, C., Branca, M.F., Weyandt, S., et al. (2016). Toll-like receptor 4-mediated

lymphocyte influx induces neonatal necrotizing enterocolitis. J. Clin. Invest. *126*, 495–508.

Egan, M., Motherway, M.O., Kilcoyne, M., Kane, M., Joshi, L., Ventura, M., and Van Sinderen, D. (2014). Cross-feeding by Bifidobacterium breve UCC2003 during co-cultivation with Bifidobacterium bifidum PRL2010 in a mucin-based medium. BMC Microbiol. *14*, 282.

Epskamp, S., Cramer, A.O.J., Waldorp, L.J., Schmittmann, V.D., and Borsboom, D. (2012). qgraph: network visualizations of relationships in psychometric data. J. Stat. Softw. *48*, 1–18.

Falony, G., Vlachou, A., Verbrugghe, K., and De Vuyst, L. (2006). Cross-feeding between *Bifidobacterium longum* BB536 and acetate-converting, butyrate-producing colon bacteria during growth on oligofructose. Appl. Environ. Microbiol. *72*, 7835–7841.

Ferrario, C., Duranti, S., Milani, C., Mancabelli, L., Lugli, G.A., Turroni, F., Mangifesta, M., Viappiani, A., Ossiprandi, M.C., Van Sinderen, D., and Ventura, M. (2015). Exploring amino acid auxotrophy in *Bifidobacterium bifidum* PRL2010. Front. Microbiol. *6*, 1331.

Ford, A.L., Nagulesapillai, V., Piano, A., Auger, J., Girard, S.A., Christman, M., Tompkins, T.A., and Dahl, W.J. (2020). Microbiota stability and gastrointestinal tolerance in response to a high-protein diet with and without a prebiotic, probiotic, and synbiotic: a randomized, double-blind, placebo-controlled trial in older women. J. Acad. Nutr. Diet. *120*, 500–516.e10.

Frese, S.A., Hutton, A.A., Contreras, L.N., Shaw, C.A., Palumbo, M.C., Casaburi, G., Xu, G., Davis, J.C.C., Lebrilla, C.B., Henrick, B.M., et al. (2017). Persistence of supplemented *Bifidobacterium longum* subsp. *infantis* EVC001 in breastfed infants. mSphere *2*. e00501-e00517.

Fukuda, S., Toh, H., Hase, K., Oshima, K., Nakanishi, Y., Yoshimura, K., Tobe, T., Clarke, J.M., Topping, D.L., Suzuki, T., et al. (2011). Bifidobacteria can protect from enteropathogenic infection through production of acetate. Nature *469*, 543–547.

Gloor, G.B., and Reid, G. (2016). Compositional analysis: a valid approach to analyze microbiome high-throughput sequencing data. Can. J. Microbiol. *62*, 692–703.

Gotoh, A., Katoh, T., Sakanaka, M., Ling, Y., Yamada, C., Asakuma, S., Urashima, T., Tomabechi, Y., Katayama-Ikegami, A., Kurihara, S., et al. (2018). Sharing of human milk oligosaccharides degradants within bifidobacterial communities in faecal cultures supplemented with Bifidobacterium bifidum. Sci. Rep. *8*, 13958.

Gu, Z., Eils, R., and Schlesner, M. (2016). Complex heatmaps reveal patterns and correlations in multidimensional genomic data. Bioinformatics *32*, 2847–2849.

Harrison, E., Drake, T., and Ots, R. (2020). finalfit: quickly create elegant regression results tables and plots when modelling. R package version 1.0.2. https://CRAN.R-project.org/package=finalfit.

Henderickx, J.G.E., Zwittink, R.D., Van Lingen, R.A., Knol, J., and Belzer, C. (2019). The preterm gut microbiota: an inconspicuous challenge in nutritional neonatal care. Front. Cell. Infect. Microbiol. *9*, 85.

Henrick, B.M., Rodriguez, L., Lakshmikanth, T., Pou, C., Henckel, E., Arzoomand, A., Olin, A., Wang, J., Mikes, J., Tan, Z., et al. (2021). Bifidobacteria-mediated immune system imprinting early in life. Cell *184*, 3884–3898.e11.

Højsgaard, S., Halekoh, U., and Yan, J. (2006). The R Package geepack for generalized estimating equations. J. Stat. Soft. *15*, 1–11.

Hothorn, T., Bretz, F., and Westfall, P. (2008). Simultaneous inference in general parametric models. Biom. J. *50*, 346–363.

Hu, H.J., Zhang, G.Q., Zhang, Q., Shakya, S., and Li, Z.Y. (2017). Probiotics prevent *Candida* colonization and invasive fungal sepsis in preterm neonates: a systematic review and meta-analysis of randomized controlled trials. Pediatr. Neonatol. *58*, 103–110.

Iannone, R. (2020). DiagrammeR: graph/network visualization. R package version 1.0.6.1. https://CRAN.R-project.org/package=DiagrammeR.

Ihrmark, K., Bödeker, I.T., Cruz-Martinez, K., Friberg, H., Kubartova, A., Schenck, J., Strid, Y., Stenlid, J., Brandström-Durling, M., Clemmensen, K.E., et al. (2012). New primers to amplify the fungal ITS2 region–evaluation by 454-sequencing of artificial and natural communities. FEMS Microbiol Ecol *82* (3), 666–677.

Kassambara, A., Kosinski, M., and Biecek, P. (2020). survminer: drawing survival curves using 'ggplot2'. R package version 0.4.8. https://CRAN.R-project.org/package=survminer.

Kline, R.B. (2016). Principles and Practices of Structural Equation Modeling (The Guilford Press).

Koenig, J.E., Spor, A., Scalfone, N., Fricker, A.D., Stombaugh, J., Knight, R., Angenent, L.T., and Ley, R.E. (2011). Succession of microbial consortia in the developing infant gut microbiome. Proc. Natl. Acad. Sci. USA *108*, 4578–4585.

Korpela, K., Blakstad, E.W., Moltu, S.J., Strommen, K., Nakstad, B., Ronnestad, A.E., Braekke, K., Iversen, P.O., Drevon, C.A., and De Vos, W. (2018). Intestinal microbiota development and gestational age in preterm neonates. Sci. Rep. *8*, 2453.

Kozich, J.J., Westcott, S.L., Baxter, N.T., Highlander, S.K., and Schloss, P.D. (2013). Development of a dual-index sequencing strategy and curation pipeline for analyzing amplicon sequence data on the MiSeq Illumina sequencing platform. Appl. Environ. Microbiol. *79*, 5112–5120.

Kuhn, M. (2020). caret: classification and regression training. R package version 6.0-86. https://CRAN.R-project.org/package=caret.

La Rosa, P.S., Warner, B.B., Zhou, Y., Weinstock, G.M., Sodergren, E., Hall-Moore, C.M., Stevens, H.J., Bennett, W.E.,J.R., Shaikh, N., Linneman, L.A., et al. (2014). Patterned progression of bacterial populations in the premature infant gut. Proc. Natl. Acad. Sci. USA *111*, 12522–12527.

Laforest-Lapointe, I., and Arrieta, M.C. (2017). Patterns of early-life gut microbial colonization during human immune development: an ecological perspective. Front. Immunol. *8*, 788.

Lee, E.K., Ahn, Y.T., Huh, C.S., Soo Kim, H., Kim, E., Chun, Y.H., Yoon, J.S., Kim, H.H., and Tack Kim, J. (2015). The early intestinal microbiota of healthy Korean newborns. Iran. J. Pediatr. *25*, e2079.

Lee, J.Y., Sohn, K.H., Rhee, S.H., and Hwang, D. (2001). Saturated fatty acids, but not unsaturated fatty acids, induce the expression of cyclooxygenase-2 mediated through Toll-like receptor 4. J. Biol. Chem. *276*, 16683–16689.

Li, N., Yan, F., Wang, N., Song, Y., Yue, Y., Guan, J., Li, B., and Huo, G. (2020). Distinct gut microbiota and metabolite profiles induced by different feeding methods in healthy Chinese infants. Front. Microbiol. *11*, 714.

Liaw, A., and Wiener, M. (2002). Classification and regression by randomForest. R News *2*, 18–22.

Maheshwari, A., Schelonka, R.L., Dimmitt, R.A., Carlo, W.A., Munoz-Hernandez, B., Das, A., Mcdonald, S.A., Thorsen, P., Skogstrand, K., Hougaard, D.M., et al. (2014). Cytokines associated with necrotizing enterocolitis in extremely-low-birth-weight infants. Pediatr. Res. *76*, 100–108.

Manzoni, P., Mostert, M., Leonessa, M.L., Priolo, C., Farina, D., Monetti, C., Latino, M.A., and Gomirato, G. (2006). Oral supplementation with *Lactobacillus casei* subspecies rhamnosus prevents enteric colonization by Candida species in preterm neonates: a randomized study. Clin. Infect. Dis. *42*, 1735–1742.

Martínez, I., Maldonado-Gomez, M.X., Gomes-Neto, J.C., Kittana, H., Ding, H., Schmaltz, R., Joglekar, P., Cardona, R.J., Marsteller, N.L., Kembel, S.W., et al. (2018). Experimental evaluation of the importance of colonization history in early-life gut microbiota assembly. eLife *7*, e36521.

Masi, A.C., and Stewart, C.J. (2019). The role of the preterm intestinal microbiome in sepsis and necrotising enterocolitis. Early Hum. Dev. *138*, 104854.

Mcmurdie, P.J., and Holmes, S. (2013). phyloseq: an R package for reproducible interactive analysis and graphics of microbiome census data. PLoS One *8*, e61217.

Melamud, E., Vastag, L., and Rabinowitz, J.D. (2010). Metabolomic analysis and visualization engine for LC-MS data. Anal. Chem. *82*, 9818–9826.

Mihi, B., Gong, Q., Nolan, L.S., Gale, S.E., Goree, M., Hu, E., Lanik, W.E., Rimer, J.M., Liu, V., Parks, O.B., et al. (2021). Interleukin-22 signaling attenuates necrotizing enterocolitis by promoting epithelial cell regeneration. Cell Rep. Med. *2*, 100320.

Milborrow, S. (2019). rpart.plot: plot 'rpart' models: an enhanced version of 'plot.rpart'. R package version 3.0.8. https://CRAN.R-project.org/package=rpart.plot.

Mitchell, C.M., Mazzoni, C., Hogstrom, L., Bryant, A., Bergerat, A., Cher, A., Pochan, S., Herman, P., Carrigan, M., Sharp, K., et al. (2020). Delivery mode affects stability of early infant gut microbiota. Cell Rep. Med. *1*, 100156.

Modi, N. (2014). Probiotics and necrotising enterocolitis: the devil (as always) is in the detail. Neonatology *105*, 71–73.

Murata, M., and Kawanishi, S. (2004). Oxidative DNA damage induced by nitrotyrosine, a biomarker of inflammation. Biochem. Biophys. Res. Commun. *316*, 123–128.

Nilsson, R.H., Larsson, K.H., Taylor, A.F.S., Bengtsson-Palme, J., Jeppesen, T.S., Schigel, D., Kennedy, P., Picard, K., Glöckner, F.O., Tedersoo, L., et al. (2019). The UNITE database for molecular identification of fungi: handling dark taxa and parallel taxonomic classifications. Nucleic Acids Res. *47*, D259–D264.

O'Callaghan, A., and Van Sinderen, D. (2016). Bifidobacteria and their role as members of the human gut microbiota. Front. Microbiol. *7*, 925.

Ofek Shlomai, N., Deshpande, G., Rao, S., and Patole, S. (2014). Probiotics for preterm neonates: what will it take to change clinical practice? Neonatology *105*, 64–70.

Oksanen, J., Blanchet, F.G., Friendly, M., Kindt, R., Legendre, P., Mcglinn, D., Minchin, P.R., O'Hara, R.B., Simpson, G.L., Solymos, P., et al. (2017). Vegan: community ecology package. R package version 2.4-3.

Olin, A., Henckel, E., Chen, Y., Lakshmikanth, T., Pou, C., Mikes, J., Gustafsson, A., Bernhardsson, A.K., Zhang, C., Bohlin, K., and Brodin, P. (2018). Stereotypic immune system development in newborn children. Cell *174*, 1277–1292.e14.

Palarea-Albaladejo, J., and Martín-Fernández, J.A. (2015). zCompositions—R package for multivariate imputation of left-censored data under a compositional approach. Chemom. Intell. Lab. Syst. *143*, 85–96.

Pammi, M., Cope, J., Tarr, P.I., Warner, B.B., Morrow, A.L., Mai, V., Gregory, K.E., Kroll, J.S., Mcmurtry, V., Ferris, M.J., et al. (2017). Intestinal dysbiosis in preterm infants preceding necrotizing enterocolitis: a systematic review and meta-analysis. Microbiome *5*, 31.

Pang, Z., Chong, J., Zhou, G., De Lima Morais, D.A., Chang, L., Barrette, M., Gauthier, C., Jacques, P.É., Li, S., and Xia, J. (2021). MetaboAnalyst 5.0: narrowing the gap between raw spectra and functional insights. Nucleic Acids Res. *49*, W388–W396.

Partida-Rodriguez, O., Nieves-Ramirez, M., Laforest-Lapointe, I., Brown, E.M., Parfrey, L., Valadez-Salazar, A., Thorson, L., Morán, P., Gonzalez, E., Rascon, E., et al. (2021). Exposure to parasitic protists and helminths changes the intestinal community structure of bacterial communities in a cohort of mother-child binomials from a semirural setting in Mexico. mSphere *6*, e0008321.

Pekár, S., and Brabec, M. (2018). Generalized estimating equations: a pragmatic and flexible approach to the marginal GLM modelling of correlated data in the behavioural sciences. Ethology *124*, 86–93.

Plummer, E.L., Bulach, D.M., Murray, G.L., Jacobs, S.E., Tabrizi, S.N., and Garland, S.M.; ProPrems Study Group. (2018). Gut microbiota of preterm infants supplemented with probiotics: sub-study of the ProPrems trial. BMC Microbiol. *18*, 184.

Quast, C., Pruesse, E., Yilmaz, P., Gerken, J., Schweer, T., Yarza, P., Peplies, J., and Glöckner, F.O. (2013). The SILVA ribosomal RNA gene database project: improved data processing and web-based tools. Nucleic Acids Res. *41*, D590–D596.

Ramiro-Cortijo, D., Singh, P., Liu, Y., Medina-Morales, E., Yakah, W., Freedman, S.D., and Martin, C.R. (2020). Breast milk lipids and fatty acids in regulating neonatal intestinal development and protecting against intestinal injury. Nutrients *12*, 534.

Rao, C., Coyte, K.Z., Bainter, W., Geha, R.S., Martin, C.R., and Rakoff-Nahoum, S. (2021). Multi-kingdom ecological drivers of microbiota assembly in preterm infants. Nature *591*, 633–638.

Ridlon, J.M., Harris, S.C., Bhowmik, S., Kang, D.J., and Hylemon, P.B. (2016). Consequences of bile salt biotransformations by intestinal bacteria. Gut Microbes *7*, 22–39.

Rosseel, Y. (2012). lavaan: an R package for structural equation modeling. J. Stat. Softw. *48*, 1–36.

Saiki, T., Mitsuyama, K., Toyonaga, A., Ishida, H., and Tanikawa, K. (1998). Detection of pro- and anti-inflammatory cytokines in stools of patients with inflammatory bowel disease. Scand. J. Gastroenterol. *33*, 616–622.

Sheffield, M., Mabry, S., Thibeault, D.W., and Truog, W.E. (2006). Pulmonary nitric oxide synthases and nitrotyrosine: findings during lung development and in chronic lung disease of prematurity. Pediatrics *118*, 1056–1064.

Shields-Cutler, R.R., Al-Ghalith, G.A., Yassour, M., and Knights, D. (2018). SplinectomeR enables group comparisons in longitudinal microbiome studies. Front. Microbiol. *9*, 785.

Spedicato, G.A. (2017). Discrete time Markov chains with R. R J *9*, 84–104.

Sprockett, D., Fukami, T., and Relman, D.A. (2018). Role of priority effects in the early-life assembly of the gut microbiota. Nat. Rev. Gastroenterol. Hepatol. *15*, 197–205.

Stewart, C.J., Embleton, N.D., Marrs, E.C., Smith, D.P., Nelson, A., Abdulkadir, B., Skeath, T., Petrosino, J.F., Perry, J.D., Berrington, J.E., and Cummings, S.P. (2016). Temporal bacterial and metabolic development of the preterm gut reveals specific signatures in health and disease. Microbiome *4*, 67.

Tannock, G.W. (2021). Building robust assemblages of bacteria in the human gut in early life. Appl. Environ. Microbiol. *87*, e0144921.

Team, R.C. (2017). R: A Language and Environment for Statistical Computing (R Foundation for Statistical Computing).

Therneau, T. (2020). A package for survival analysis in R. R package version 3.2-7. https://CRAN.R-project.org/package=survival.

Therneau, T., and Atkinson, B. (2019). rpart: recursive partitioning and regression trees. R package version 4.1-15. https://CRAN.R-project.org/package=rpart.

Tibshirani, R., Walther, G., and Hastie, T. (2001). Estimating the number of clusters in a data set via the gap statistic. J. R. Stat. Soc. B *63*, 411–423.

Vongbhavit, K., and Underwood, M.A. (2016). Prevention of necrotizing enterocolitis through manipulation of the intestinal microbiota of the premature infant. Clin. Ther. *38*, 716–732.

Walter, J., and Ley, R. (2011). The human gut microbiome: ecology and recent evolutionary changes. Annu. Rev. Microbiol. *65*, 411–429.

Walter, J., Maldonado-Gómez, M.X., and Martínez, I. (2018). To engraft or not to engraft: an ecological framework for gut microbiome modulation with live microbes. Curr. Opin. Biotechnol. *49*, 129–139.

Wandro, S., Osborne, S., Enriquez, C., Bixby, C., Arrieta, A., and Whiteson, K. (2018). The microbiome and metabolome of preterm infant stool are personalized and not driven by health outcomes, including necrotizing enterocolitis and late-onset sepsis. mSphere *3*. e00104-e00118.

Wilke, C.O. (2020). ggridges: ridgeline plots in 'ggplot2'. R package version 0.5.2. https://CRAN.R-project.org/package=ggridges.

Yassour, M., Vatanen, T., Siljander, H., Hämäläinen, A.M., Härkönen, T., Ryhänen, S.J., Franzosa, E.A., Vlamakis, H., Huttenhower, C., Gevers, D., et al. (2016). Natural history of the infant gut microbiome and impact of antibiotic treatment on bacterial strain diversity and stability. Sci. Transl. Med. *8*, 343ra81.

Young, T.P., Petersen, D.A., and Clary, J.J. (2005). The ecology of restoration: historical links, emerging issues and unexplored realms. Ecol. Lett. *8*, 662–673.

Zheng, J., Wittouck, S., Salvetti, E., Franz, C.M.A.P., Harris, H.M.B., Mattarelli, P., O'Toole, P.W., Pot, B., Vandamme, P., Walter, J., et al. (2020). A taxonomic note on the genus *Lactobacillus*: description of 23 novel genera, emended description of the genus *Lactobacillus* Beijerinck 1901, and union of Lactobacillaceae and Leuconostocaceae. Int. J. Syst. Evol. Microbiol. *70*, 2782–2858.

STAR★METHODS

KEY RESOURCES TABLE

REAGENT or RESOURCE	SOURCE	IDENTIFIER
Biological samples		
Fecal sample (1ml)	This study	NA
Commercial kits		
MOBIO dry bead tubes	MOBIO laboratories	Discontinued
DNeasy PowerSoil Pro Kit	Qiagen, Canada	Cat# 47016
Mesoscale kits: V-PLEX TH17 Panel 1, V-PLEX Proinflammatory Cytokine Panel 1, and R-PLEX Human Calprotectin assays	Mesoscale Discoveries	Cat # K15085D, K15049D, F21YB
Pierce BCA Protein Assay Kit	Thermo Scientific	Cat # 23225
Primers		
16S rRNA-Forward Primer GTGCCAGCMGCCGCGGTAA	Caporaso et al. (2012)	515F
16S rRNA-Reverse Primer GGACTACHVGGGTWTCTAAT	Caporaso et al. (2012)	806R
ITS2-Forward CCTCCGCTTATTGATATGC	Ihrmark et al. (2012)	ITS4
ITS2-Reverse CCGTGARTCATCGAATCTTTG	Ihrmark et al. (2012)	ITS1
FloraBABY specific qPCR primers	Table S6	
Software and algorithm		
DADA2	Callahan et al. (2016)	https://doi.org/10.1038/nmeth.3869
SILVA v.132	Quast et al. (2013)	https://doi.org/10.1093/nar/gks1219
UNITE v.8.0	Nilsson et al. (2019)	https://doi.org/10.1093/nar/gky1022
R v. 4.03	R Core Team	https://www.r-project.org
Phyloseq v. 1.32.0	McMurdie and Holmes (2013)	https://joey711.github.io/phyloseq/index.html
randomForest v.4.6-14		
CoDaSeq	Gloor and Reid (2016)	https://github.com/ggloor/CoDaSeq
Vegan v. 2.5.7	Oksanen et al. (2017)	https://cran.r-project.org/web/packages/vegan/vegan.pdf
Survival v3.2-7	Therneau (2020)	https://CRAN.R-project.org/package=survival
Lavaan v. 0.6-6	Rosseel (2012)	http://www.jstatsoft.org/v48/i02/
Markovchain v.0.8.5	Spedicato (2017)	https://journal.r-project.org/archive/2017/RJ-2017-036/index.html
SplinectomeR v.0.1.0	Shields-Cutler et al. (2018)	https://github.com/RRShieldsCutler/splinectomeR
MetaboAnalyst v. 5.0	Pang et al. (2021)	https://doi.org/10.1093/nar/gkab382
Analysis codes	Data S1	
Deposited data		
16S rRNA sequence data	This paper	NCBI BioProject: PRJNA721684
ITS2 sequencing	This paper	NCBI BioProject: PRJNA721688
Metabolomics mass spectral raw data	This paper	MetaboLights (study identifier MTBLS4056)

RESOURCE AVAILABILITY

Lead contact

Further information and requests for resources and reagents should be directed to and will be fulfilled by the lead contact, Marie-Claire Arrieta (marie.arrieta@ucalgary.ca).

Materials availability

This study did not generate new unique reagents.

Data and code availability

- Demultiplexed 16S and ITS2 sequencing data were deposited into the Sequence Read Archive (SRA) of NCBI and can be accessed via accession numbers PRJNA721684 and PRJNA721688. Metabolomics mass spectral raw data were deposited to MetaboLights (study identifier MTBLS4056). This information can also be found in the key resources table.
- The R codes are provided as Data S1.
- Any additional information required to reanalyze the data reported in this work paper is available from the Lead Contact upon request.

EXPERIMENTAL MODEL AND SUBJECT DETAILS

Inclusion and exclusion of study participants

This study was part of a randomized, open-label, controlled trial in the NICU of the Foothills Medical Centre in Calgary (ClinicalTrials.gov Identifier: NCT03422562). FloraBABY (Renew Life®, Canada) probiotic was administered to infants in the intervention arm after randomization. Eligible participants were premature infants admitted to the NICU with birth weight < 1000 grams and born at less than 29 weeks GA. Eligible infants were identified within 24 hours of birth and parents were approached for informed consent. Once consent was obtained, infants were randomly assigned in blocks of 4 to receive either FloraBABY probiotics or no product. Randomization was conducted using a computer-generated table of random numbers. The study excluded infants with major congenital anomalies, hypoxic-ischemic injury and NEC or bowel perforation occurring within 72 hours of birth. Probiotic administration was started before 7 days of age and continued until 37 weeks post-menstrual age, at a dose of 0.5g per day in 1 ml of milk or colostrum as part of the feeding. Each dose contained 4×10^9 total colony forming unit (CFU) of four *Bifidobacterium* strains (*B. breve* 1.2×10^9 CFU, *B. bifidum* 8×10^8 CFU, *B. infantis* 6×10^8 CFU, *and B. longum* 6×10^8) together with *Lacticaseibacillus* (formerly *Lactobacillus* (Zheng et al., 2020)) *rhamnosus* 1×10^9 CFU, mixed with maltodextrin and ascorbic acid. No probiotic or placebo was given to infants in the control group. Treatment for the intervention group started after obtaining informed parental consent and after the first stool sample was obtained, except for two infants, who received the probiotic before the first stool sample. Probiotics were administered until the age of term (37-39 weeks post-menstrual age). Total probiotic treatment duration ranged between 45-87 days, depending on gestational age at birth (Figure 1A). This trial was conducted in accordance and compliance with all relevant ethical regulations by the Conjoint Health Research Ethics Board of the University of Calgary (approved protocol REB16-0542).

Maternal, infant and early-life factors

The following variables were collected throughout the study and incorporated in the analysis: GA at birth, chronological age, birth weight, sex, number of older siblings, mode of delivery, maternal antenatal administration of antibiotics, age in days at the start of enteral feeds and inclusion in the study, total duration of probiotics, duration of neonatal antibiotic use (type and duration), type of feeds during NICU and up to 6 months CA, including milk type, fortification, and type of fortification (see Table S1).

METHOD DETAILS

Sample collection and processing

Stool samples were collected at five time points: prior to first probiotic administration (T1); 2-3 weeks after first administration (T2); 4-5 weeks after first probiotic administration (T3); 2 weeks after probiotic discontinued (T4); and at 6 months CA (T5; Figure 1A). CA refers to the infant age if the pregnancy would have gone to term. Stool samples for the control group were collected at matched gestational and chronological age time points. Stool was collected directly from the infant's diaper by NICU nurses (T1-T4) or participant parents at home (T5). Samples were placed at 4°C in the NICU or at home for a maximum of 12 hours, or at -20°C in a NICU or home freezer for up to 48 hours and were stored at -80°C upon arrival in the laboratory for subsequent processing.

DNA extraction

DNA was extracted from ~50 mg of stool. Samples were mechanically lysed using MO BIO dry bead tubes (MO BIO Laboratories, USA) and the FastPrep homogenizer (TissueLyser II, Qiagen, Hilden, Germany) before DNA extraction with the DNeasy PowerSoil Pro Kit according to the manufacturer's instructions (Qiagen, Canada). Following extraction, DNA concentration was measured in a NanoDrop spectrophotometer (Thermofisher, Canada) and subsequently used in qPCR and sequencing reactions.

Quantitative PCR

To specifically quantify FloraBABY strains in fecal samples, qPCR was performed on genomic DNA using specific primer sequences (Table S6) and qPCR protocols previously validated to detect these probiotic strains in stool samples (Ford et al.,

2020). We carried out further validation of the specificity of the primers using individual strains in maltodextrin powder and a standard operating procedure, provided by Lallemand Health Solutions, Montreal, Canada. Each strain powder was spiked into stool samples negative for the probiotic strains. These samples were obtained from infants enrolled in a longitudinal birth cohort study in rural Mexico, with no history of exposure to probiotics. To determine the concentration of each strain, one gram of lyophilized powder of each probiotic strain was diluted in 99 ml phosphate buffered saline to obtain 10^{-2} solution. Flow cytometry counts provided the concentration (bacteria/ml) to calculate the total count of cells in 10^{-2} solution for each strain. A selected set of stool samples from Mexican cohort were spiked with the exact volume required to reach a concentration of 10^9 bacteria/ml. Unspiked stool samples were used as negative controls. To validate the qPCR methods, ten-fold dilutions (10^2 to 10^9) of DNA extracted from the spiked and unspiked aliquots were used as templates in qPCR validation plates (triplicates for each dilution). Reactions were run using StepOne™ Real-Time PCR System using the following protocol: 2 initial steps of 2 min each at 50 °C and 95 °C, followed by 40 cycles of 15 seconds at 95 °C, 30 seconds at 60 °C and 30 seconds at 72 °C. DNA concentrations were measured for all five probiotic strains using serially diluted spiked DNA extracted from spiked stool samples as standards. Clinical samples were run on duplicate using 4ng of extracted DNA as template. Cell numbers were calculated as cell/ml based on the standard curve method. Cell number values obtained below the detection limit (10^3 cells/ml for all probiotic strains) were substituted with limit of detection divided by square root of 2 to account for variance in statistical tests and models.

16S rRNA and ITS2 gene sequencing

PCR was used to amplify the V4 region of the bacterial 16S rRNA gene and the ITS2 region of the fungal ITS genetic marker from fecal DNA. This generated ready-to-pool dual-indexed amplicon libraries as described previously (Kozich et al., 2013). 16S and ITS amplicon libraries were prepared at Microbiome Insights (University of British Columbia, Vancouver, Canada). In-house extracted DNA samples were sent to the facility and amplified using Phusion Hot Start II DNA Polymerase (Thermo-Fisher). PCR products were purified, and DNA concentration normalized using the high-throughput SequalPrep Normalization Plate Kit (Applied Biosystems, USA) and quantified accurately with the KAPA qPCR Library Quantification kit (Roche, Canada). Controls without template DNA and mock communities with known amounts of selected bacteria and fungi were included in the PCR and downstream sequencing steps to control for microbial contamination and verify bioinformatics analysis pipeline. Samples were sequenced in two runs and biological controls were included in both runs to assess for batch effects. The pooled and indexed libraries were denatured, diluted, and sequenced in paired-end modus on an Illumina MiSeq (Illumina Inc., San Diego, USA). 16S rRNA and ITS2 gene sequencing were performed at Microbiome Insights, Vancouver, BC.

Metabolomics

Untargeted fecal metabolomics was performed at the Metabolomics Research Facility of the University of Calgary. Stool samples from timepoints 1, 3, 4 and 5 (N=209) were prepared for metabolomic analysis. Frozen fecal samples were mixed with ice-cold 50% methanol in a 1:5 ratio and homogenized in a bead beater with three small steel beads (30Hz for 2x1.5 minute) using high quality 2mL autoclaved safe-lock tubes. Samples were incubated for 30 min at 4 °C and then centrifuged for 10 min at maximum speed at 4 °C. The supernatant was collected and stored at -80 °C until analysis. 200uL of each sample were transferred to 0.8mL deep 96-well plates. Prior to the run samples were diluted further to 1:50. Samples were run on a Q Exactive™ HF Hybrid Quadrupole-Orbitrap™ Mass Spectrometer (Thermo-Fisher, Catalog number: IQLAAEGAAPFALGMBFZ) coupled to a Vanquish™ UHPLC System Integrated biocompatible system (Thermo-Fisher, Catalog number: IQLAAAGABHFAPUMZZZ (Chernikova et al., 2018)). Chromatographic separation was achieved on a Syncronis HILIC UHPLC column (2.1mm × 100mm × 1.7μm, Thermo-Fisher) using a binary solvent system at a flow rate of 600uL/min. Solvent A consisted of 20mM ammonium formate pH 3.0 in mass spectrometry grade H_2O; Solvent B, mass spectrometry grade acetonitrile with 0.1% formic acid (%v/v). The following gradients were used: 0-2 mins, 100% B; 2-7 mins, 100-80% B; 7-10 mins, 80-5% B; 10-12 mins, 5% B; 12-13 mins, 5-100% B; 13-15 mins, 100% B. A sample injection volume of 2μL was used. The mass spectrometer was run in negative full scan mode at a resolution of 240,000 scanning from 50-750m/z. Metabolite data were analyzed using the MAVEN software packages (Clasquin et al., 2012; Melamud et al., 2010). Metabolites were identified by matching observed m/z signals (+/- 10ppm) and chromatographic retention times to those observed from commercial metabolite standards (Sigma). Creatine was quantified by an 8-point standard curve. Metabolomic data were normalized by median, square root transformed, and pareto scaled (mean-centered and divided by the square root of the standard deviation of each variable) using Metaboanalyst 5.0 (Pang et al., 2021) for downstream analysis.

Immune factor determination

Frozen stool samples were used to measure cytokine, chemokine and calprotectin concentrations using the V-PLEX TH17 Panel 1, V-PLEX Proinflammatory Cytokine Panel 1, and R-PLEX Human Calprotectin assays (Mesoscale Devices). Prior to assay determination, 50 – 150 mg of sample were homogenized in 1 mL of lysis buffer (150 mM NaCl, 20 mM Tris, 1 mM EGTA, 1% Triton X-100, protease inhibitor) for 4 min at 20 Hz using a tissue homogenizer (TissueLyser II, Qiagen). Homogenized samples were then centrifuged at 14,000 x g for 10 min to removed debris, and appropriately diluted according to total protein present in corresponding supernatants, as determined by the Pierce BCA Protein Assay Kit (Thermo Scientific, Product No. 23225). Acquired MSD data for each sample was then normalized to its total protein concentration prior to statistical analysis.

QUANTIFICATION AND STATISTICAL ANALYSIS

Statistical details (methods, software, sample size and variance metrics) of all experiments and data analyses is provided in this section, as well as in figure legends and results section.

Sequencing processing

Sequences were checked for quality, trimmed, merged, and checked for chimeras using the *DADA2* v1.10.1 (Callahan et al., 2016) pipelines for 16S or ITS2. Unique amplicon sequence variants (ASVs) were assigned taxonomy using the UNITE v.8.0 (fungi) (Nilsson et al., 2019) and SILVA v.132 (bacteria) (Quast et al., 2013) databases at 99% sequence similarity. Sequencing data analysis was conducted in R (Team, 2017). Initial preprocessing of the ASV table was conducted using the *Phyloseq* package v.1.26.1 (McMurdie and Holmes, 2013). Overall, 10,915 unique bacterial ASVs were detected. ASVs only present in the negative controls (n=3,963) and ASVs belonging to phylum Cyanobacteria, family of mitochondria, and class of chloroplast (n=49) were removed. Samples with less than 5,000 sequencing reads were excluded (n=15) and ASVs with less than 20 reads across the entire dataset (n=6,173) were also removed. The remaining samples (n=264) were rarefied to the minimum 6,000 sequencing reads per sample resulting in 3,410 remaining ASVs. This dataset was used for analysis unless otherwise specified. For the ITS2 dataset, 3,400 unique ASVs were detected. ASVs only present in the negative controls (n=29) and ASVs belonging to kingdom Plantae (n=53) and unclassified fungi at phylum level (n=815) were removed. Samples with less than 5,000 sequencing reads were excluded (n=15) and ASVs with less than 20 reads across the entire dataset were also removed resulting in 2,319 remaining ASVs. This dataset was used for analysis unless otherwise specified.

Assessing sequencing technical accuracy

Genomic DNA of 6-8 samples was included in sequencing library preparation of both sequencing runs as biological controls. We assessed the technical accuracy between the runs by analyzing biological controls composition between the runs (Figures S1A and S1B). Depth of sequencing was also compared between the sequencing runs. Run 2 had significantly higher sequencing depth per sample in both 16S rRNA and ITS2 gene sequencing (Figures S1C and S1D). Run 2 included a higher proportion of older infants and had higher total DNA concentration (Figures S1E and S1F). No other variables differed between sequencing runs.

Exclusion of data

Two infants received probiotics prior to sample collection and thus their T1 samples were removed from the analysis.

Probiotic *strain* colonization assessment

Data analysis was conducted in R v.4.0.3 (Team, 2017). The effect of the probiotic intervention and sampling timepoint on probiotic strain cell number was determined using linear mixed models (LMM) and post estimation for linear combination of coefficients using *lme4* v.1.1.26 (Bates et al., 2015), *foreign* v.0.8.80 and *multcomp* v.1.4.16 (Hothorn et al., 2008) packages. The frequency of probiotic strains detection at different timepoints were compared between controls and infants who received the probiotic using χ^2 test.

Identification of microbiome community types

Microbiome maturation was assessed using hierarchical clustering on Bray-Curtis dissimilarity matrix at the genus level, with ward sum-of-square algorithm. The optimal number of clusters was determined using Gap statistics, which compares the observed change in within-cluster dispersion versus the expected change under an appropriate reference null distribution (Tibshirani et al., 2001). Dissimilarity (β-diversity) of clusters was assessed by permutational ANOVA (PERMANOVA) using the *vegan* package v.2.5.7 (Oksanen et al., 2017).

Assessment of the effect of probiotics on the transition to the mature community type

Markov chain state transition probabilities were estimated using *markovchain* package v.0.8.5 (Spedicato, 2017) and visualized using *DiagrammeR* v.1.0.6.1 (Iannone, 2020). The time to transition to the mature community type was assessed using Kaplan Meyer analysis using *survival* package v.3.2.7 and visualized by *survminer* package v.0.4.8 (Therneau, 2020; Kassambara et al., 2020). The confounding effect of other relevant early life events on the association of probiotics with gut microbiome maturation was assessed using logistic regression using *finalfit* package v.1.0.2 (Harrison et al., 2020).

Comparison of microbiome composition in preterm with term infants

Comparison of preterm and term infant gut microbiome was performed using the gut microbiome data of a preliminary subset of term infants enrolled in the MAGIC Study (ClinicalTrials.gov Identifier: NCT03001167), a longitudinal microbiome study of term infants conducted at the Children's Hospital of Philadelphia. We focused on breastfed, vaginally-born term infants at 1 week (N=44) and 6 months (N=24) of age. Clustering as explained above was applied to the term infant data at the genus level and compositional dissimilarity was assessed using Bray-Curtis metric and visualized using *ggridges* package v. 0.5.2 (Wilke, 2020). The difference in PCoA1 was calculated for the preterm infants to the mean of PCoA1 of terms infants at 1week and compared based on the intervention using ANOVA. The microbiome composition at the genus level was z normalized and visualized in a heatmap using *ComplexHeatmap* package v. 2.4.2 (Gu et al., 2016).

Ecological investigation of microbiome community in response to probiotics

Microbiome network analysis was conducted at the genus level and separately for each cluster. Genera with less that 0.1% mean relative abundance and less than 25% prevalence were excluded. The microbiome data was centre log-ratio transformed to control for compositionality (Palarea-Albaladejo and Martin-Fernandez, 2015; Gloor and Reid, 2016). Subsequently, partial correlations were assessed using Spearman rank correlation and correlations with absolute coefficient of more than 0.25 were visualized as networks using *qgraph* package v. 1.6.5 (Epskamp et al., 2012). Centrality network parameters were estimated using *qgraph* package (Epskamp et al., 2012).

Metabolomics comparison by intervention and community type

Differential metabolic features were identified using MetaboAnalyst 5.0 with volcano plot, using a fold change threshold of 2 and adjusted t-test threshold of 0.05 (Pang et al., 2021).

Predictive modelling

Predictive modelling was conducted to identify predictors of microbiome maturation in premature infants. Decision tree was performed using *rpart* v. 4.1.15 and visualized using *rpart.plot* v. 3.0.8 (Therneau and Atkinson, 2019; Milborrow, 2019). Random forest was performed using 10-fold cross-validation, 500 trees, and 1000 permutation using *randomForest* v. 4.6.14 and *caret* v. 6.0.86 packages (Liaw and Wiener, 2002; Kuhn, 2020).

Structural equation modelling

Structural equation modeling (SEM) was performed using the *lavaan* package v. 0.6.6 (Rosseel, 2012). The model was estimated using maximum likelihood (ML) parameter estimation and NLMINB optimization method with bootstrapping (n=1000) (Kline, 2016). Model fit was assessed by χ^2 test, the comparative fix index (CFI), root mean square error of approximation (RSMEA) and its 90% confidence interval (CI), and the standardized root mean residuals (SRMR). Non-significant χ^2 test, CFI $\geq$ 0.9, RMSEA<0.05, and SRMR<0.08 were considered as indications of good model fit (Kline, 2016).

Longitudinal analysis

Longitudinal analysis was performed using permuspliner function from splinectomeR v.0.1.0 with 1000 permutations (Shields-Cutler et al., 2018) for taxa, and generalized estimating equation (GEE) (Pekár and Brabec, 2018) for cytokines using geepack v.1.3.2 (Højsgaard et al., 2006). The optimum GEE model for each cytokine was selected based on the cytokine distribution and the model performance with different correlation structures: independence, exchangeable, autoregressive 1, or unstructured. The family of the GEE model was set as gaussian or gamma for normal or positively skewed cytokine distribution, respectively. The models were compared based on the quasi-likelihood information (QIC) criterion using MuMIn v.1.43.17 and pander v.0.6.4 packages (Bartoń, 2020; Daróczi and Tsegelskyi, 2018). The model with the lowest QIC was selected for each cytokine. Trend analysis was conducted using trendyspliner function of SplinectomeR.

Univariate analysis of cytokines and metabolites

Cytokine and metabolite concentrations were compared by pairwise Wilcoxon test.

ADDITIONAL RESOURCES

ClinicalTrials.gov identifier: NCT03422562.